Conclusions

4. CONCLUSIONS

1. S'han sintetitzat cinc nous carborans zwitteriònics de fórmula general 7-R^1-8-R^2-10-SR_2-7,8-$C_2B_9H_{11}$ en els quals el compensador de càrrega és un grup sulfoni situat en el B(10).

2. S'ha estudiat la termòlisi dels carborans zwitteriònics 10-SMe_2-7,8-$C_2B_9H_{11}$ (**2a**), 10-SEt_2-7,8-$C_2B_9H_{11}$ (**2b**) i 10-$S(CH_2)_4$-7,8-$C_2B_9H_{11}$ (**2c**) en xilè i mesitilè.

2a. En cada cas s'obté una mescla en diferents proporcions del compost 2,3-$C_2B_9H_{11}$ (**4**) i de l'isòmer **1a**, **1b** ó **1c**, de fórmula general 9-SR_2-7,8-$C_2B_9H_{11}$, segons fóra el producte de partida **2a**, **2b** ó **2c**, respectivament.

2b. S'ha dut a terme un seguiment de la cinètica de la reacció de termòlisi dels carborans zwitteriònics **2a**, **2b** i **2c** mitjançant ^{11}B RMN. D'aquesta manera ha estat possible determinar que l'espècie **4** és originada per la termòlisi de l'isòmer **1**; tanmateix, no és possible concloure si l'isòmer **2** també pot originar l'espècie **4**, o bé si és imprescindible una prèvia isomerització a l'isòmer **1**.

2c. La termòlisi controlada de l'isòmer **2**, amb el grup sulfoni en el B(10), en un dissolvent aromàtic amb una temperatura de reflux adequada és un mètode de síntesi viable de cara a obtenir el respectiu isòmer **1**, amb el grup sulfoni en el B(9), amb un rendiment quantitatiu.

2d. La termòlisi dels carborans zwitteriònics **2** en un dissolvent aromàtic amb una temperatura de reflux suficientment elevada és un mètode de síntesi viable de cara a obtenir el compost 2,3-$C_2B_9H_{11}$ (**4**) amb una conversió quantitativa.

3. El mètode més adequat per la desprotonació dels carborans zwitteriònics **2** i **3** és en un dissolvent tipus alcohol i emprant ^{t}BuOK com a base. Aquestes condicions de reacció són més suaus que les usades pels seus isòmers posicionals **1**, i permeten facilitar els posteriors passos de complexació amb metalls i separació de les mescles de reacció.

4. S'ha trobat un mètode general per la síntesi dels complexos de tipus semi-sandvitx de ruteni de fórmula general [1-R^1-3-H-3,3-$(PPh_3)_2$-8-L-3,1,2-$RuC_2B_9H_9$], per reacció dels carborans monoaniònics amb $[RuCl_2(PPh_3)_3]$. Aquest mètode sintètic s'ha utilitzat per preparar els complexos **21a-f** i **31a-b**.

5. S'ha trobat un mètode general per la síntesi dels complexos de tipus semi-sandvitx de rodi de fórmula general [1-R^1-3,3-$(PPh_3)_2$-8-L-3,1,2-$RhC_2B_9H_9$], per reacció dels carborans monoaniònics amb el catalitzador de Wilkinson. Aquest mètode sintètic s'ha utilitzat per preparar els complexos **22a-f** i **32a**. En utilitzar el mètode amb el carborà zwitteriònic **2a** i el complex $[\{Rh(cod)Cl\}_2]$ com a font del metall s'obté el complex [3,3-cod-8-SMe_2-3,1,2-$RhC_2B_9H_{10}$] (**23a**).

6. Els complexos **22a-d** han mostrat un comportament singular quan es dissolen en determinats dissolvents clorats.

6a. Quan el dissolvent és $CHCl_3$, CCl_4 o $ClCH_2$-CH_2Cl, es dóna l'evolució cap a la formació de nous complexos de fórmula general [3,3-Cl_2-3-PPh_3-8-L-3,1,2-$RhC_2B_9H_9$] (**22A-D**). S'han observat diferents velocitats de reacció en funció del compost clorat. Contràriament, quan el dissolvent és CH_2Cl_2 o un compost aromàtic clorat, no es dóna cap tipus de transformació.

6b. S'ha proposat un mecanisme de tipus radicalari per la transformació de **22a-d** a **22A-D** que concorda amb totes les dades aportades per les experiències de ^{31}P, ^{11}B, ^{1}H, ^{13}C RMN i EPR.

7. La reacció del carborà zwitteriònic **2a** desprotonat, en presència d'un halur de metall amb els lligands adients, porta a la formació del corresponent complex de tipus sandvitx (**24a-28a**). L'àtom metàl·lic se situa sempre entre les cares pentagonal obertes de dos carborans monoaniònics **2a**, amb una rotació relativa dels dos lligands depenent del metall complexat.

7a. El mètode semiempíric ZINDO/1 ha permès calcular el perfil rotacional dels complexos **24a-28a**, d'on se'n deriven les conformacions teòricament més estables per a cadascun dels complexos. Les orientacions relatives entre lligands trobades concorden amb les dades cristal·logràfiques.

7b. Les barreres rotacionals calculades experimentalment pels complexos **24a-28a** mitjançant estudis de RMN a baixa temperatura han donat suport als perfils calculats de forma teòrica.

7c. L'estudi dels processos electroquímics accessibles que es donen en els complexos **24a-28a** han mostrat que la capacitat electrodonadora del carborà monoaniònic **2a** és inferior tant a la del dianió dicarbollur com a la de l'anió ciclopentadienur.

7d. El complex catiònic de tipus sandvitx de cobalt, **24a**, s'ha utilitzat com a element bàsic en materials supramoleculars en combinació amb el radical orgànic 7,7,8,8-Tetracianoquinodimetà i amb l'anió [3,3'-Co(1-PPh_2-1,2-$C_2B_9H_{10})_2]^-$.

8. Els complexos **21a-f** i **22a-f** s'han aplicat com a precursors catalítics en la ciclopropanació d'olefines i els resultats s'han contrastat amb els d'altres complexos que contenen lligands η^5 i presenten una estructura similar [$RuClCp^{\#}(PPh_3)_2$] ($Cp^{\#}$=Cp (**41**), Cp* (**42**), Indenil (**43**)).

8a. Els rutenacarborans (**21a-f**) i els rodacarborans (**22a-f**) catalitzen la ciclopropanació d'estirè a 80 ºC amb uns rendiments del corresponent ciclopropà del 90-96 % i 72-87 %, respectivament. L'estereoselectivitat d'ambdós famílies de catalitzadors és *trans*.

8b. Els complexos **21a-f** catalitzen la ciclopropanació d'estirè i derivats a una temperatura d 40 ºC amb uns rendiments del corresponent ciclopropà del 80-85 % i una estereoselectivitat *anti*. D'entre els complexos **41-43**, el complex **41** és l'únic que mostra uns rendiments similars als dels rutenacarborans, encara que amb una regioselectivitat inversa.

8c. Les dades experimentals suporten que el cicle catalític predominant en la ciclopropanació d'olefines catalitzada pels complexos **21a-f** és el mateix que els dels complexos **41-43**. La via proposada suposa la formació d'un intermedi ciclobutànic de Ru^{IV} l'estabilitat del qual depèn de les propietats electròniques del lligand η^5.

9. Els complexos **21a-f** i **22a-f** s'han aplicat com a precursors catalítics en l'addició Kharasch de CCl_4 a una sèrie d'olefines representatives i els resultats s'han contrastat amb els d'altres complexos que contenen lligands η^5 i presenten una estructura similar $[RuClCp^{\#}(PPh_3)_2]$ ($Cp^{\#}$=Cp (**41**), Cp* (**42**), Indenil (**43**)), entre els quals es troben els millors catalitzadors basats en ruteni coneguts fins al moment.

9a. Els rutenacarborans (**21a-f**) catalitzen l'addició Kharasch de CCl_4 a totes les olefines provades a 40 ºC amb uns rendiments excel·lents. Les seves activitats i selectivitats són superiors a la dels catalitzadors **41-43**, passant a ser, per tant, els millors catalitzadors descrits fins al moment basats en ruteni per l'addició de Kharasch. Per l'altra banda, els rodacarborans (**22a-f**) no són uns bons precursors per a aquesta reacció, mostrant una marcada tendència a l'oligomerització i polimerització dels substrats.

9b. S'ha proposat una relació entre el potencial redox d'oxidació dels complexos de ruteni estudiats i la seva activitat catalítica. Per a aquest tipus de complexos s'ha trobat una zona de potencials on l'activitat presentada és màxima.

10. Els complexos de ruteni (**21a-f** i **31a-b**) i els de rodi (**22a-f** i **32a**) s'han aplicat com a precursors catalítics en la polimerització ATRP d'una sèrie d'olefines representatives i els resultats s'han contrastat amb els d'altres complexos que contenen lligands η^5 i presenten una estructura similar $[RuClCp^{\#}(PPh_3)_2]$ ($Cp^{\#}$=Cp (**41**), Cp* (**42**), Indenil (**43**)), entre els quals es troben els millors catalitzadors basats en ruteni coneguts fins al moment.

10a. Els rutenacarborans (**21a-f**) catalitzen la polimerització ATRP de totes les olefines provades a 110 ºC, tanmateix la reacció no és controlada en cap dels casos. S'ha cercat una relació entre el potencial redox d'oxidació dels complexos de ruteni estudiats i la seva eficiència. Els complexos en què el centre metàl·lic és més difícilment oxidable són els que han mostrat les millors eficiències.

10b. Els rodacarborans (**22a-f** i **32a**) catalitzen la polimerització ATRP de totes les olefines provades a 110 ºC, tanmateix la falta de control és encara més acusada que en els rutenacarborans.

11. S'han sintetitzat els carborans zwitteriònics neutres de fórmula general 7,10-$(SMe_2)_2$-8-R-7,8-$C_2B_9H_8$ (**5a-b**) els quals presenten dos grups sulfoni com a compensadors de càrrega. La seva protonació porta a l'obtenció d'un dels pocs exemples disponibles d'un carborà catiònic.

12. S'ha sintetitzat un complex de Rh^I amb el carborà zwitteriònic neutre 5a per reacció amb una solució de $[Rh(cod)]^+$. Les dades cristal·logràfiques han mostrat que es dóna una isomerització del carboni substituït amb el grup sulfoni en el procés de complexació. Experiències complementàries han demostrat que la temperatura no és la causa d'aquest reordenament.

Articles publicats

(Comissió de Doctorat d'abril de 2003)

ELSEVIER

Journal of Organometallic Chemistry 657 (2002) 247–255

Journal of Organometallic Chemistry

www.elsevier.com/locate/jorganchem

Recent studies on $RR'S \cdot C_2B_9H_{11}$ charge-compensated ligands Crystal structures of 10-$(S(CH_3)_2)$-7,8-$C_2B_9H_{11}$ and 10-$(S(CH_2)_4)$-7,8-$C_2B_9H_{11}$

Oscar Tutusaus [a], Francesc Teixidor [a,*], Rosario Núñez [a], Clara Viñas [a], Reijo Sillanpää [b], Raikko Kivekäs [c]

[a] *Institut de Ciència de Materials de Barcelona, Campus de la U.A.B. CSIC, E-08193 Bellaterra, Spain*
[b] *Department of Chemistry, University of Jyväskylä, FIN-40351 Jyväskylä, Finland*
[c] *Department of Chemistry, University of Helsinki, PO Box 55, FIN-00014 Helsinki, Finland*

Received 31 July 2001; accepted 23 April 2002

Abstract

In this paper we report the synthesis of three new carborane derivatives of the series 7,8-R,R'-10-L-7,8-$C_2B_9H_9$ (R = R' = H, L = SEtPh; R = CH_3, R' = H, L = SMe_2 and L = SEt_2) along with the enhanced characterization of formerly described compounds 7,8-R,R'-10-L-7,8-$C_2B_9H_9$ (R = R' = H, L = SMe_2 (**1**), L = SEt_2 (**2**) and L = $S(CH_2)_4$ (**3**)). They have been fully characterised using ^{1}H-, ^{11}B- and ^{13}C-NMR spectroscopy. Their bridging proton resonances have been located for the first time. Individual sulfonium substituent contributions have been calculated that have permitted to establish a rule to predict its position in the ^{1}H-NMR spectrum. The crystal structures of **1** and **3** have been resolved for the first time. Thermolysis of **1**, **2** and **3** in aromatic solvents at reflux temperature yielded a mixture of the corresponding 9-substituted derivative via isomerisation and 2,3-*closo*-$C_2B_9H_{11}$ via elimination of SR_2. This reaction has been demonstrated to be tuneable upon convenient choice of the aromatic solvent, the ligand and the reaction time, leading to a new and more straightforward preparation of the series 9-L-7,8-*nido*-$C_2B_9H_{11}$ and the cluster 2,3-*closo*-$C_2B_9H_{11}$.

Keywords: Zwitterionic clusters; Cluster's isomerization; Nido-carboranylmonosulfonium; Cluster's thermolisis

1. Introduction

The dicarbollide dianions, $[7,8\text{-}C_2B_9H_{11}]^{2-}$ and $[7,9\text{-}C_2B_9H_{11}]^{2-}$, have been extensively used as ligands in organometallic chemistry because of their similarities with the cyclopentadienide ion, $[C_5H_5]^-$, to which are formally isolobal [1]. To certain extent, this analogy is enough to establish comparisons however, discrepancies have been observed as a result of the higher negative charge of the dicarbollide anion. A proper comparison would be with isomeric monoanionic charge-compensated ligands of the type $[LC_2B_9H_{10}]^-$ (L = pyridine, THF, SR_2, PPh_3, OEt_2, etc.) derived from both dicarbollide dianions [2]. Known charge-compensated carborane ligands derived from the *o*-carborane are those of general formula 7-L-8-R-7,8-$C_2B_9H_{10}$, 7-R^1-8-R^2-9-L-7,8-$C_2B_9H_9$, and 7,8-R_2-10-L-7,8-$C_2B_9H_9$ in which the charge-compensating substituent (L) is located on the 7, 9 or 10-position of the open face, respectively (Fig. 1a). On the other hand, isomers derived from the *m*-carborane are also known (Fig. 1b).

The procedure to prepare 10-substituted charge-compensated ligands containing a sulfonium group 10-L-7,8-$C_2B_9H_{11}$ (L = SR_2) has been described by Plesek et al. by treating the *nido*-carborane with the corresponding sulfide in the presence of CH_3CHO and acid [2d]. To prepare the 9-substituted isomer, 9-L-7,8-$C_2B_9H_{11}$, two different methods have been reported: the first one is restricted to L = SMe_2, and consists in the

* Corresponding author. Tel.: +34-93-5801853; fax: +34-93-5805729
E-mail address: teixidor@icmab.es (F. Teixidor).

0022-328X/02/$ - see front matter
PII: S0022-328X(02)01541-3

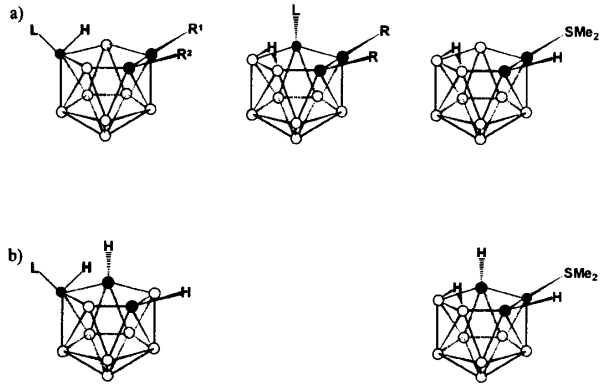

Fig. 1. Schematic representation of the charge-compensated carborane compounds derived from the *o*- and *m*-carborane.

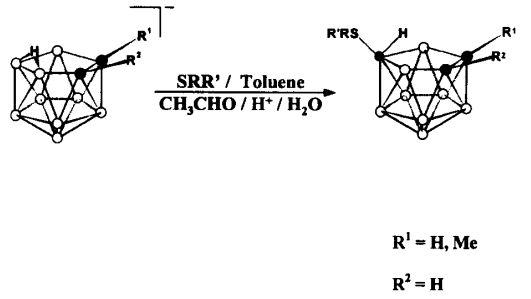

Scheme 1. General reaction for preparing charge-compensated sulfide carborane ligands.

reaction of the *nido*-carborane with DMSO in water in strong acidic media [2b,3] and the second one which is adequate for different L groups, involves the ferric chloride-driven oxidative coupling reaction of [*nido*-7,8-$C_2B_9H_{12}$]$^-$ with an electron pair donor (L) [4]. The last one, however, leads to a mixture of both isomers 9-L-7,8-$C_2B_9H_{11}$ and 10-L-7,8-$C_2B_9H_{11}$ in different ratios depending on L. On the other hand, the 10-L-7,9-$C_2B_9H_{11}$ isomer has been prepared directly by the reaction of *closo*-2,3-$C_2B_9H_{11}$ with L in benzene [2a,5].

In this paper we report the synthesis of three new 10-substituted charge-compensated carborane derivatives and the bridging proton resonances of the previously synthesized [10-L-7,8-$C_2B_9H_{11}$] (L = SRR′) which had not been located in other examples of the series reported. Besides, individual sulfonium substituent contributions have been calculated and a rule has been established to predict its position in the ^{1}H-NMR. Also, a new way to get asymmetric 9-substituted isomers and the 2,3-*closo*-$C_2B_9H_{11}$ by thermolysis of 10-substituted ligands, in aromatic solvents at reflux temperature, is reported. It is also demonstrated that the reaction is fully tuneable upon convenient choice of the temperature and the reaction time.

2. Results and discussion

2.1. Synthesis and characterization of charge-compensated carborane ligands 7-R-10-L-7,8-$C_2B_9H_{10}$

The reaction of K[7-R-7,8-$C_2B_9H_{11}$] (R = H, Me) with SRR′ in the presence of acid and CH_3CHO leads to the formation of charge-compensated carborane ligands.

Following the known Plesek's et al. [2d] procedure (see Scheme 1) 10-SMe_2-7,8-$C_2B_9H_{11}$ (**1**), 10-SEt_2-7,8-$C_2B_9H_{11}$ (**2**), 10-$S(CH_2)_4$-7,8-$C_2B_9H_{11}$ (**3**), and the new ligands 10-SEtPh-7,8-$C_2B_9H_{11}$ (**4**), 7-Me-10-SMe_2-7,8-$C_2B_9H_{10}$ (**5**) and 7-Me-10-SEt_2-7,8-$C_2B_9H_{10}$ (**6**) have been synthesized. All compounds were obtained in good yield as white solids and were fully characterized by elemental analysis and NMR spectroscopies corroborating their formation.

The ^{1}H-NMR spectra of all these charge-compensated ligands show a broad resonance in the negative region, between −0.97 and −1.26 ppm, which collapses to a singlet in the ^{1}H{^{11}B}-NMR spectra. This signal is, in fact, a broad quadruplet due to the ^{1}H–^{11}B coupling (ca. 75 Hz), probably with the B10. This was unexpected since Plesek et al. [2d] previously reported that no sign of B–H–B bridge signal had been found for compounds **1**, **2** and **3**. This resonance is observed at lower field than in non-charge-compensated *nido*-carboranes (ca. −2.50 ppm), perhaps providing some hints about the acidity of the proton. For compounds **1**, **2**, **3** and **4**, broad singlets of intensity 2 were observed between 2.23 and 2.19 ppm, which were assigned to the cage C–H protons. For **5** and **6**, which have a methyl on one carbon cluster, the corresponding C–H signal is found at higher field, 2.11 and 2.10 ppm, respectively. The ^{1}H-NMR spectra of **1** and **5** showed one singlet assigned to the S–CH_3 group. For compounds **2**, **3**, **4** and **6** the S–CH_2 protons are chemically non-equivalent, which is reflected in the ^{1}H-NMR spectra. Two J(H, H) coupling constants, one for the geminal protons (^2J(H, H) ca. 13.5 Hz) and a second one for the neighbor CH_3 or CH_2 protons (^3J(H, H) ca. 7 Hz) were observed. Something similar was already observed by Welch and co-workers in compounds 7,8-Ph_2-10-(SMeEt)-7,8-*nido*-$C_2B_9H_9$ and 7,8-Ph_2-10-SEt_2-7,8-*nido*-$C_2B_9H_9$ [2f]. The ^{13}C{^{1}H}-NMR spectra in addition to the resonances due to the substituents on the molecule, displayed broad resonances in the region between 42.6 and 59.8 ppm, which were attributed to the cluster carbon atoms. The ^{11}B{^{1}H}-NMR spectra of all compounds appear in the region −10.0– −37.0 ppm. Compounds **1**, **2** and **3** display very similar ^{11}B{^{1}H}-NMR spectra showing a six signal 2:2:1:2:1:1 pattern and suggesting a C_s molecular symmetry. Nevertheless, the presence of two different groups bonded to the

sulfur atom, in compound **4**, destroys the C_s symmetry, causing the splitting of one resonance of intensity 2 into two 1:1 [2f]. The $^{11}B\{^1H\}$-NMR spectra of compounds **5** and **6** reflect the molecule asymmetry producing a 1:1:1:2:1:1:1:1 pattern. All these compounds display a resonance near −26 ppm, which has been attributed to the L-substituted B10 atom based on the ^{11}B- and $^{11}B\{^1H\}$-NMR looks. The ^{11}B spectrum of **1**, **2** and **3** was already assigned in the literature by $^{11}B\{^1H\}$–$^{11}B\{^1H\}$ correlated spectroscopy. To assign the ^{11}B resonances of the new compounds **4**, **5** and **6** to specific boron atoms 2D-COSY NMR espectra were performed. This has permitted to draw the diagrams shown in Fig. 2. The asymmetry introduced substituting the 7-position, has modified considerably the look of the spectrum, as shown in Fig. 3.

2.2. *Molecular structures of 10-SMe_2-7,8-nido-$C_2B_9H_{11}$ and 10-$S(CH_2)_4$-7,8-nido-$C_2B_9H_{11}$*

Although 10-SMe_2-7,8-$C_2B_9H_{11}$ (**1**) and 10-$S(CH_2)_4$-7,8-$C_2B_9H_{11}$ (**3**) had been long ago synthesized by Plesek et al. [2d] their molecular geometry had been assigned only by spectroscopic methods. Considering the relevance these compounds may have as alternatives to Cp, efforts were made to get good crystals suitable of X-ray analysis. In this regard crystals of **1** and **3** were obtained from a solution of chloroform/hexane in a 1/1 ratio.

X-ray analyses of **1** and **3** confirmed that the SMe_2 and $S(CH_2)_4$ substituents are connected to B10 of the *nido* carborane cage. Some selected bond parameters for **1** and **3** and perspective drawings of the ligands are shown in Figs. 4 and 5.

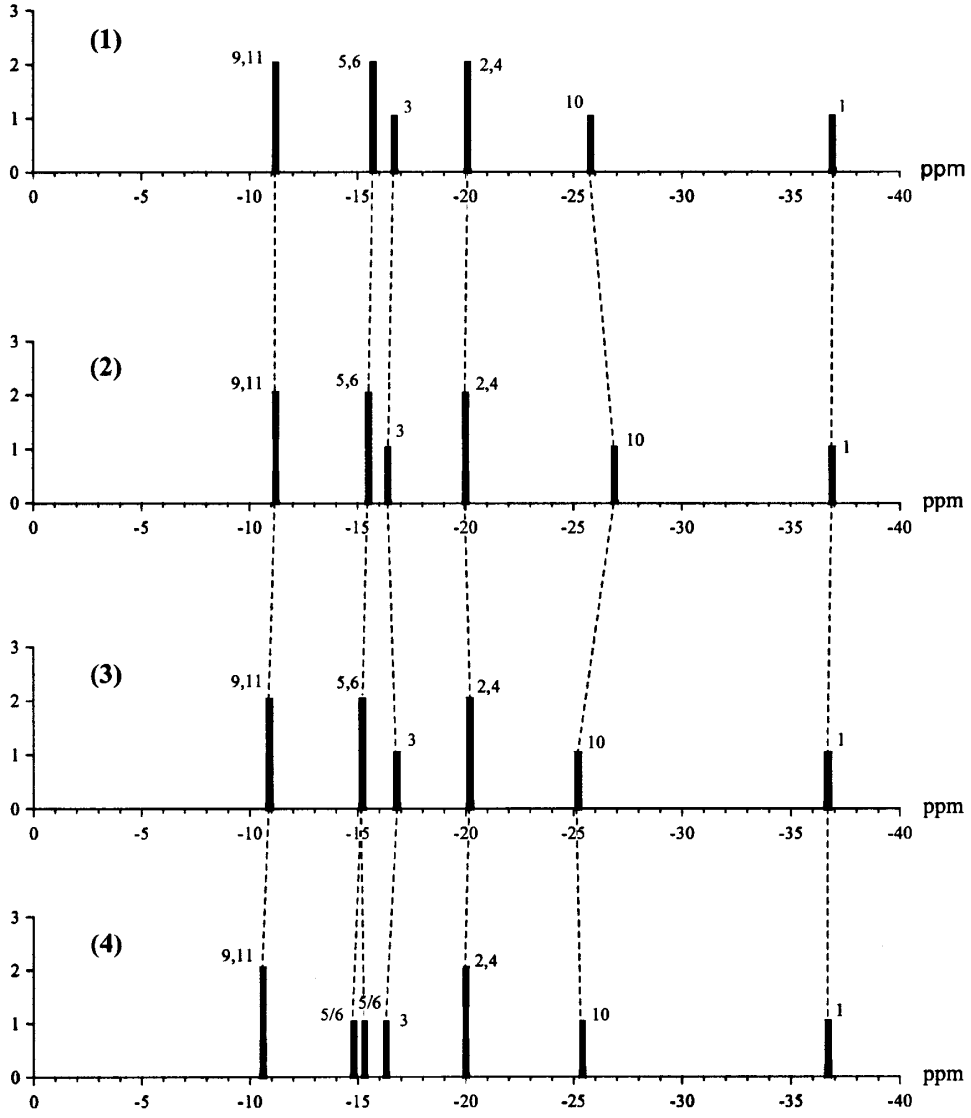

Fig. 2. Representation of the $^{11}B\{^1H\}$ resonances for compounds **1**, **2**, **3** and **4**.

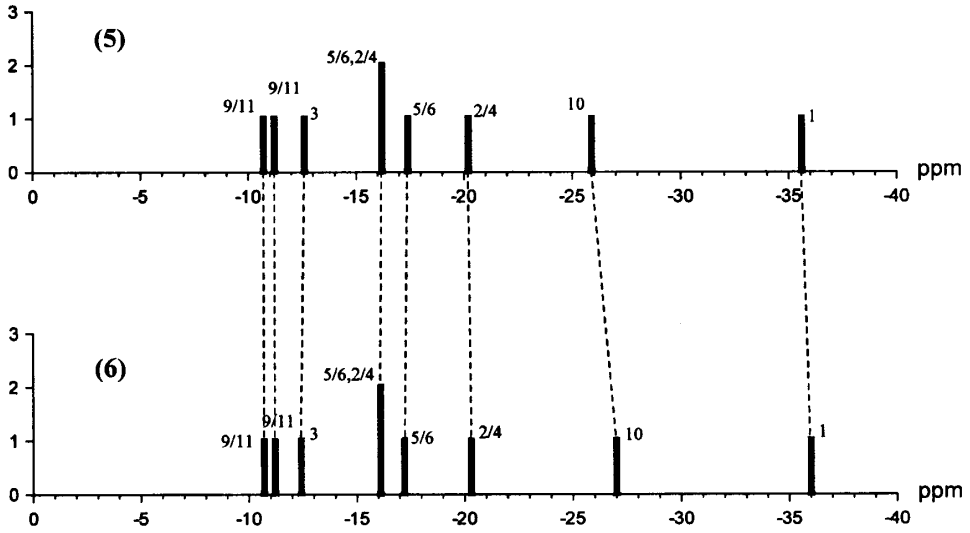

Fig. 3. Representation of the $^{11}B\{^1H\}$ resonances for compounds **5** and **6**.

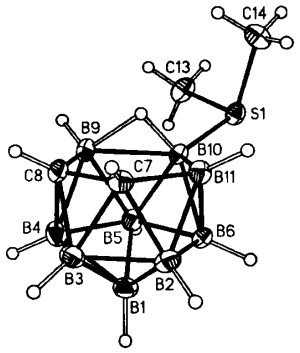

Fig. 4. Perspective drawing of compound **1**. Selected bond lengths (Å) and angles and torsion angles (°): S1–B10 1.895(3), S1–C13 1.804(3), S1–C14 1.798(3), C8–B9 1.612(4), B9–B10 1.853(4), B10–B11 1.792(4), B10–S1–C13 104.01(13), B10–S1–C14 102.92(13), S1–B10–B9 126.05(18), B11–B10–S1 124.35(19), B9–B10–S1–C13 –11.1(3), B11–B10–S1–C14 –55.3(2), C7–C8 1.547(4) distance.

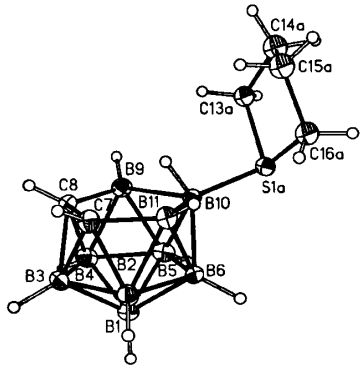

Fig. 5. Simplified drawing of compound **3**. Conformation **B** of the disordered $S(CH_2)_4$ group, having minor occupancy, is omitted. Selected bond lengths (Å) and angles and torsion angles (°): S1a–B10 1.888(4), S1a–C13a 1.833(5), S1a–C16a 1.806(5), C8–B9 1.594(5), B9–B10 1.819(6), B10–B11 1.835(5), C13a–S1a–C16a 94.8(2), B10–S1a–C13a 104.4(2), S1a–B10–B9 122.8(3), S1a–B10–B11 130.4(3), B9–B10–S1a–C13a 39.0(4), B11–B10–S1a–C16a –17.7(4), C7–C8 1.546(5) distance.

In **1**, mutual orientation of the methyl groups with respect to the C_2B_3 open face are different as indicated by the B9–B10–S1–C13 and B11–B10–S1–C14 torsion angle values of –11.1(3) and –55.3(2)°, respectively. Lengthening of the B9–B10 bond (1.853(4) Å) compared with the B10–B11 bond (1.792(4) Å) can be attributed to the orientation of the methyl group C13. The B9–B10 edge carries an asymmetric H-bridge with bond distances B10–H10 = 1.18(2) and B9–H10 = 1.42(2) Å.

In **3**, the $S(CH_2)_4$ ring is disordered assuming two conformations (**A** and **B**) with site occupation parameters 0.773(7) and 0.227(7). The two conformations are partly superimposed and oriented so that the sulphur lone pair of electrons is *anti* to the C_2B_3 open face. Bond lengths to S1 in **1** and **3** agree well with the comparable distances in 9-SMe_2-7,8-$C_2B_9H_{11}$ [6], 7-Ph-11-SMe_2-7,8-$C_2B_9H_{10}$ [2e] and 7,8-Ph_2-10-SMe_2-7,8-$C_2B_9H_9$ [2f] and the C7–C8 distances of 1.547(4) and 1.546(5) Å in **1** and **3** fall in the range normally found for the *nido*-cages bearing H atoms at the cluster carbons.

Nature of the hydrogen atoms at B10 in compounds **1** and **3** is clearly different. In **1** H10 is bridging between B10 and B9 but in **3** H10 is terminal with the B10–H10, B9···H10 and B11···H10 distances of 1.10(3), 1.83(3) and 1.67(3) Å, respectively.

2.3. Prediction of the B–H–B chemical shift for charge-compensated ligands in the ^{1}H-NMR

The B–H–B chemical shift in charge-compensated ligands 10-SRR′-7-R1-8-R2-7,8-$C_2B_9H_{11}$ has been shifted to lower field with regard to their *nido-o*-carborane derivative precursors (Table 1). This could be expected considering that in 10-SRR′-7,8-$C_2B_9H_{11}$ the open face proton is mainly located on the B10 atom which has an electron-withdrawing substituent (SRR'^+). Therefore the B–H–B chemical shift in the ^{1}H-NMR will be affected by changes on B10 and, given the case, its position in the ^{1}H-NMR spectrum could be calculated by considering additive individual contributions. Indeed this seems to work this way and the chemical shifts can be reasonably well calculated. Table 2 contains the calculated contribution of each group, which appears to be independent of the different starting *nido-o*-carborane derivative whether it is *o*-carborane or methyl-*o*-carborane. The computed individual values permit us to predict the B–H–B chemical shift for other charge-compensated carborane ligands, that otherwise could be difficult to be distinguished in the ^{1}H-NMR spectrum due to the overlap with other cluster B–H protons. In this regard, Welch and co-workers [2f] have prepared charge-compensated ligands derivatives of the 7,8-Ph_2-7,8-$C_2B_9H_{10}$ for which the open face B–H–B position in the ^{1}H-NMR has not been discussed. The B–H–B chemical shifts of these compounds in the ^{1}H-NMR spectra therefore could be calculated by using the additive method suggested here (see Table 1).

2.4. Isomerization by the temperature

Thermolysis of **1**, **2** and **3** in mesitylene (b.p. = 163 °C) and xylene (b.p. = 140 °C) at refluxing temperature has been carried out and monitored (see Tables 3 and 4). Scheme 2 shows the results of the thermolysis of **2** in mesitylene for 1 h, which leads to the formation of two compounds. No attempt was made to isolate the new generated species however, they were identified in solution by ^{11}B{^{1}H}-NMR. The two species were 9-SEt_2-7,8-$C_2B_9H_{11}$ (**7**) and the cluster *closo*-2,3-$C_2B_9H_{11}$ (**8**). We can extend this procedure to other members of the series finding that the rate and ratio of products obtained depend on the starting compound, the solvent used, and the reaction time.

Thermolysis of **1**, **2** and **3** in mesitylene was followed by ^{11}B{^{1}H}-NMR spectroscopy (see Section 3). Again, the rate and percentage of isomerization in these compounds depends clearly on the substituent (SR_2) bonded to the B10 atom in the cluster. For (**1**) (L = SMe_2) the reaction is very fast (see Fig. 6) and after 40 min, the starting compound has been completely converted into the isomer 9-SMe_2-7,8-$C_2B_9H_{11}$ (**9**) and the *closo*-species (**8**) in a ratio 32:68, respectively. We can also observe that after 5 h of reaction only the *closo*-species (**8**) is in solution (Fig. 7). This implies that the *closo*-species is generated from **9**, however, we do not have any conclusive evidence whether **8** can also be generated directly from the 10-substituted isomer **1**. For (**2**) (L = SEt_2) the reaction is slower as after 2 h there is a 1:1 formation of **7** and **8**. When the reaction is left to go for several hours, the 9-substituted isomer **7** is trans-

Table 1
Experimental and predicted B–H–B chemical shift in the ^{1}H-NMR spectrum for charge-compensated carborane compound [10-L-7-R^1-8-R^2-7,8-$C_2B_9H_9$]

L	R^1	R^2	δ_{B-H-B} (ppm)	Predicted δ (ppm)
–H	H	H	−2.90	–
–Sme_2	H	H	−1.17	−1.17
–SEt_2	H	H	−1.26	−1.26
–$S(CH_2)_4$	H	H	−1.19	−1.19
–SEtPh	H	H	−0.98	−0.98
–H	CH_3	H	−2.71	–
–Sme_2	CH_3	H	−0.97	−0.98
–SEt_2	CH_3	H	−1.07	−1.07
–H	Ph	Ph	−1.71	–
–Sme_2	Ph	Ph	–	0.02
–SMeEt	Ph	Ph	–	−0.02
–SEt_2	Ph	Ph	–	−0.07

Table 2
Individual contribution of the sulfonium substituent ($\Delta\delta$) B–H–B chemical shift in the ^{1}H-NMR spectrum

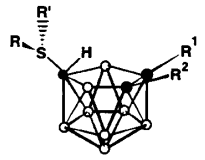

Substituents R/R′	$\Delta\delta$ (ppm)
–Me	0.86
–Et	0.82
–$(CH_2)_2$–	0.85
–Ph	1.10

Table 3
Thermolysis of ligands **1**–**3** in xylene

Time (min)	Ligand **1**		Ligand **2**		Ligand **3**	
	% **9**	% **8**	% **7**	% **8**	% **10**	% **8**
10	5	1	3	0	3	0
40	12	9	8	0.5	12	0
120	22	46	23	3	32	0
300	28	66	47	6	58	0

Percentage of 9-isomers and 2,3-*closo*-$C_2B_9H_{11}$ at different times.

Table 4
Thermolysis of ligands **1**–**3** in mesitylene

Time (min)	Ligand **1**		Ligand **2**		Ligand **3**	
	% **9**	% **8**	% **7**	% **8**	% **10**	% **8**
10	31	25	15	15	33	2
40	35	65	48	40	74	6
120	19	81	49	49	83	11
300	7	93	–	–	79	16

Percentage of 9-isomers and 2,3-*closo*-$C_2B_9H_{11}$ at different times.

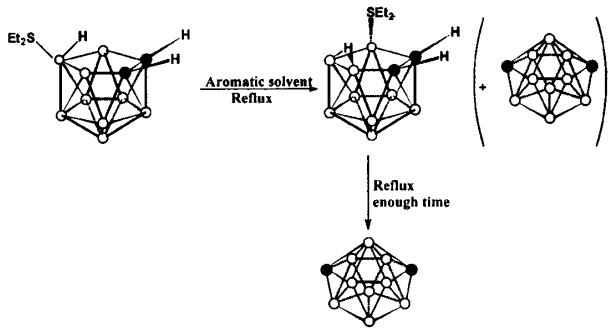

Scheme 2. Isomerization of 10-SEt_2-7,8-$C_2B_9H_{11}$ in aromatic solvents.

formed to **8**. Compound (**3**) (L = $S(CH_2)_4$) behaves a little bit different mainly producing the 9-isomer [9-$S(CH_2)_4$-7,8-$C_2B_9H_{11}$] (**10**) (83%) after 2 h of thermolysis, however, as for the other members (given enough time), it is transformed into the *closo*-species.

No difference is observed when **1** is refluxed in xylene, since it leads to the same results as those obtained in mesitylene although, in this case, the reaction occurs more slowly. Different results have been obtained for **2** and **3**. In both cases, the reaction leads mainly to 9-substituted isomers, a 90% for ligand **2** and 100% for ligand **3**. For the latter, no formation of *closo*-species (**8**) is observed at any time as can be observed from the graphic in Fig. 8.

Zakharkin et al. had described positional isomerization by protonation/deprotonation reaction [7]. The procedure reported in this paper is based on sulfonium derivatives while Zakharkin's was applied only to alkyl derivatives. Similar conditions leaded to the *closo*-2,3-$C_2B_9H_{11}$ from [7,9-$C_2B_9H_{12}$]$^-$ in a 36% yield [2a]. Nevertheless, the best synthetic method till now was by thermolysis of [Ni(7,8-$C_2B_9H_{12})_2$] at 300 °C in a nitrogen atmosphere with a 41% yield [2b].

As a conclusion, it appears that open face positional isomers of X-SRR′-7-R^1-8-R^2-7,8-$C_2B_9H_9$ (X = 9, 10) can be synthesized according to the needs. Probably the 10-SRR′-isomer is the kinetically more stable while the 9-SRR′-isomer is the thermodynamically preferred. Therefore controlled thermolysis of 10-SRR′-isomer leads to the respective 9-SRR′-isomer. However, when

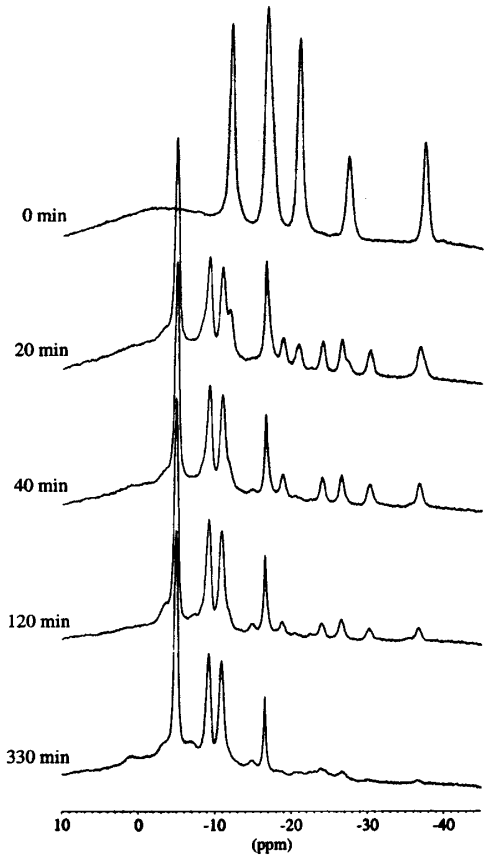

Fig. 6. $^{11}B\{^1H\}$-NMR spectra corresponding to the thermolysis reaction of **1** in mesitylene at different times.

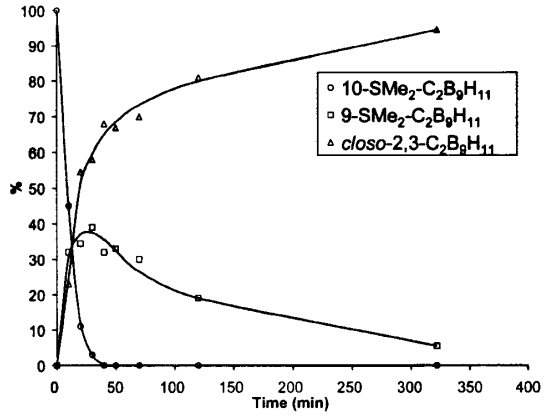

Fig. 7. Thermolysis of compound **1** in mesitylene.

$R^1 = R^2 = H$, the latter is susceptible to undergo SRR′ cleavage followed by a rearrangement to *closo*-2,3-$C_2B_9H_{11}$. It is thus clear that *closo*-2,3-$C_2B_9H_{11}$ originates from 9-SRR′-isomer, but we cannot rule out that, additionally, it may also be originated from the 10-SRR′-isomer. By tuning up the reaction conditions, mainly the temperature, the 9-SRR′-isomers free of *closo*-2,3-$C_2B_9H_{11}$ can be synthesized. These studies

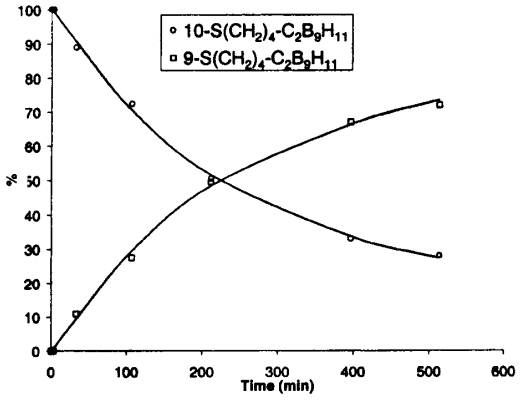

Fig. 8. Thermolysis of compound **3** in xylene.

bring about the possibility to generate different positional isomers with different substituents, and we expect that the method can be of general use. These compounds have the same charge as the Cp or Cp* and can find a good application in catalysis.

We believe that the thermolysis procedure reported here can be precisely controlled and should permit easy reproducibility.

3. Experimental

3.1. Instrumentation

Microanalyses were performed in our analytical laboratory using a Carlo Erba EA1108 microanalyser. IR spectra (ν, cm^{-1}; KBr pellets) were obtained on a Nicolet 710-FT spectrophotometer. The ^1H- (300.13 MHz), ^{11}B- (96.29 MHz), and $^{13}C\{^1H\}$-NMR (75.47 MHz) spectra were obtained on a Bruker ARX 300 instruments. All NMR measurements were performed in $CDCl_3$ at 22 °C. The ^{11}B-NMR shifts are referenced to external $BF_3 \cdot O(Et)_2$, while the δ ^1H and ^{13}C data are referenced to $Si(Me)_4$. Chemical shifts are reported in units of parts per million (ppm). According to the IUPAC convention, positive values of the chemical shifts are to high frequency. All coupling constant values are reported in Hertz.

3.2. Materials

Before use, 1-methyl-*o*-carborane and *o*-carborane (Katchem Ltd. Prague) were sublimed under high vacuum. The 1 M aqueous solution of potassium 7,8-dicarba-*nido*-undecaborate and potassium 7-methyl-7,8-dicarba-*nido*-undecaborate were prepared from *o*-carborane and methyl-*o*-carborane, respectively, according to the method reported previously [8]. The thioethers SMe_2, SEt_2, $S(CH_2)_4$ from Fluka and SEtPh, ^{t}BuOK and CH_3CHO from Aldrich were used as purchased. 10-SMe_2-7,8-*nido*-$C_2B_9H_{11}$ (**1**), 10-SEt_2-7,8-*nido*-$C_2B_9H_{11}$ (**2**) and 10-$S(CH_2)_4$-7,8-*nido*-$C_2B_9H_{11}$ (**3**) were synthesized by standard literature methods [2d]. Although compounds **1–3** have been already synthesized and characterized, no complete details on their spectroscopic characterization had been reported. These data are reported here. Diethyl ether and $C_6H_5CH_3$ were dried with Na/benzophenone and distilled. EtOH, C_6H_{14} and $CHCl_3$ were dried with molecular sieves. Unless mentioned elsewhere, all reactions were carried out under N_2 atmosphere and used solvents were oxygen free and dry.

3.3. Characterization of 10-SMe_2-7,8-nido-$C_2B_9H_{11}$ (1)

Following the method described by Plesek et al. [2d], compound **1** was obtained. IR: ν 3014 (C_c–H); 2924 (C–H); 2542 (B–H). ^1H-NMR: δ −1.17 (br quadruplet, 1H, ^1J(B, H) = 74, B–H–B); 2.23 (br s, 2H, C_c–H); 2.56 (s, 6H, CH_3). ^{11}B-NMR: δ −11.2 (d, 2B, ^1J(B, H) = 144, B(9,11)); −15.7 (d, 2B, ^1J(B, H) = 131, B(5,6)); −16.7 (d, 1B, ^1J(B, H) = 166, B(3)); −20.1 (d, 2B, ^1J(B, H) = 156, B(2,4)); −25.8 (d, 1B, ^1J(B, H) = 74, B(10)); −36.9 (d, 1B, ^1J(B, H) = 144, B(1)). $^{13}C\{^1H\}$-NMR: δ 26.5 (s, CH_3); 46.9 (br s, C_c–H).

3.4. Characterization of 10-SEt_2-7,8-nido-$C_2B_9H_{11}$ (2)

Following the method described by Plesek et al. [2d], compound **2** was obtained. IR: ν 3028 (C_c–H); 2970, 2936, 2875 (C–H); 2539 (B–H). ^1H-NMR: δ −1.26 (br quadruplet, 1H, ^1J(B, H) = 79, B–H–B); 1.56 (dd, 6H, $^3J(H_a, H) = 7.0$, $^3J(H_b, H) = 7.6$, CH_3); 2.23 (br s, 2H, C_c–H); 2.90 (dq, 2H, $^2J(H_a, H_b) = 13.5$, $^3J(H_a, H) = 7.0$, S–CH_a (S–CH_2)); 3.02 (dq, 2H, $^2J(H_b, H_a) = 13.5$, $^3J(H_b, H) = 7.6$, S–CH_b (S–CH_2)). ^{11}B-NMR: δ −11.2 (d, 2B, ^1J(B, H) = 142, B(9,11)); −15.5 (d, 2B, ^1J(B, H) = 131, B(5,6)); −16.4 (d, 1B, ^1J(B, H) = 173, B(3)); −20.0 (d, 2B, ^1J(B, H) = 156, B(2,4)); −26.9 (d, 1B, ^1J(B, H) = 79, B(10)); −36.9 (d, 1B, ^1J(B, H) = 146, B(1)). $^{13}C\{^1H\}$-NMR: δ 11.8 (s, CH_3); 34.9 (s, S–CH_2); 46.7 (br s, C_c–H).

3.5. Characterization of 10-$S(CH_2)_4$-7,8-nido-$C_2B_9H_{11}$ (3)

Following the method described by Plesek et al. [2d], compound **3** was obtained. IR: ν 3029 (C_c–H); 2940, 2865 (C–H); 2521 (B–H). ^1H-NMR: δ −1.19 (br quadruplet, 1H, ^1J(B, H) = 79, B–H–B); 2.10 (m, 2H, CH_2); 2.21 (br s, 2H, C_c–H); 2.35 (m, 2H, CH_2); 3.30 (m, 4H, S–CH_2). ^{11}B-NMR: δ −10.9 (d, 2B, ^1J(B, H) = 143, B(9,11)); −15.2 (d, 2B, ^1J(B, H) = 138, B(5,6)); −16.8 (d, 1B, ^1J(B, H) = 167, B(3)); −20.2 (d, 2B, ^1J(B, H) = 156, B(2,4)); −25.2 (d, 1B, ^1J(B, H) = 79, B(10)); −36.7 (d, 1B, ^1J(B,H) = 144, B(1)). $^{13}C\{^1H\}$-

NMR: δ 30.4 (s, CH_2); 43.7 (s, S–CH_2); 46.7 (br s, C_c–H).

3.6. Synthesis of 10-SEtPh-7,8-nido-$C_2B_9H_{11}$ (4)

Following the method of Plesek et al. [2d], to a two-necked round bottom flask (25 ml) containing a cooled and stirring 1 M aqueous solution of [K][7,8-$C_2B_9H_{12}$] (5 ml), were added dropwise SEtPh (2.8 ml, 20 mmol) in $C_6H_5CH_3$ (5 ml) and concd. HCl (2.5 ml). The mixture was vigorously stirred for 5 min to turn slightly orange. After this time, 16% aq. CH_3CHO (3.75 ml) was added. After stirring for 4 h, the organic phase was separated and water (7.5 ml) was added. The solution was evaporated at room temperature, and the solid formed was extracted with $CHCl_3$ (5 ml). Compound **4** was purified on flash chromatopraphy on silica using $CHCl_3$ as eluent. Removal of solvent afforded **1** as a white solid. Yield: (478 mg, 35%). Anal. Calc. for $C_{10}H_{21}B_9S$ (%): C, 44.41; H, 7.77; S, 11.84. Found: C, 44.12; H, 7.56; S, 11.02. IR: ν 3051 (C_{aryl}–H); 2979, 2936, 2869 (C–H); 2545 (B–H). ^{1}H-NMR: δ −0.98 (br quadruplet, 1H, B–H–B); 1.26 (t, 32 H, ^3J(H, H) = 7.4, CH_3); 2.19 (br s, 2H, C_c–H); 3.30 (m, 4H, S–CH_2); 7.72 (m, 5H, S–C_6H_5). ^{11}B-NMR: δ −12.2 (d, 2B, ^1J(B, H) = 140, B(9,11)); −16.2 (d, 1B, ^1J(B, H) = 135); −16.9 (d, 1B), −17.8 (d, 1B, ^1J(B, H) = 119); −21.5 (d, 2B, ^1J(B, H) = 147); −26.9 (d, 1B, B(10)); −38.2 (d, 1B, ^1J(B, H) = 143). ^{13}C{^{1}H}-NMR: δ 12.0 (s, CH_3); 39.4 (s, S–CH_2); 46.6 (br s, C_c–H); 126.1 (s, C_{aryl}); 131.2 (s, C_{aryl}); 132.1 (s, C_{aryl}); 133.3 (s, C_{aryl}).

3.7. Synthesis of 7-Me-10-SMe_2-7,8-nido-$C_2B_9H_{10}$ (5)

The same procedure was used as before, using SMe_2 (1.2 ml, 16 mmol) in $C_6H_5CH_3$ (4 ml), concd. HCl (2 ml), 1 M aqueous solution of [K][7,8-$C_2B_9H_{12}$] (4 ml) and 16% aq. CH_3CHO (3 ml). After stirring for 4 h, the organic phase was evaporated and extracted with $CHCl_3$. The solid formed was dissolved in $CHCl_3$ and purified by flash chromatography on silica, using $CHCl_3$ as eluent. Compound **5** was obtained as a white solid. Yield: (592 mg, 63%). Anal. Calc. for $C_5H_{19}B_9S$ (%): C, 28.82; H, 9.13; S, 15.37. Found: C, 29.05; H, 8.89; S, 14.99. IR ν: 3016 (C_c–H); 2953, 2926, 2868 (C–H); 2544 (B–H). ^{1}H-NMR: δ −0.97 (br quadruplet, 1H, ^1J(B, H) = 77, B–H–B); 1.49 (s, 3H, CH_3); 2.11 (br s, 1H, C_c–H); 2.55 (s, 6H, CH_3). ^{11}B-NMR: δ −10.7 (d, 1B, ^1J(B, H) = 141); −11.2 (d, 1B, ^1J(B, H) = 143); −12.6 (d, 1B, ^1J(B, H) = 162); −16.2 (d, 2B, ^1J(B, H) = 148); −17.4 (d, 1B, ^1J(B, H) = 138); −20.2 (d, 1B, ^1J(B, H) = 156); −25.9 (d, 1B, ^1J(B, H) = 77); −35.9 (d, 1B, ^1J(B, H) = 143). ^{13}C{^{1}H}-NMR: δ 24.7 (s, CH_3); 25.8 (s, CH_3); 52.6 (br s, C_c–H).

3.8. Synthesis of 7-Me-10-SEt_2-7,8-nido-$C_2B_9H_{10}$ (6)

The same procedure was used as before, using SEt_2 (2.2 ml, 20 mmol) in $C_6H_5CH_3$ (5 ml), concd. HCl (2.5 ml), 1 M aqueous solution of [K][7,8-$C_2B_9H_{12}$] (5 ml) and 16% aq. CH_3CHO (3.75 ml). After stirring for 4 h, the organic phase was evaporated and extracted with $CHCl_3$. The solid formed was dissolved in $CHCl_3$ and purified by flash chromatography on silica, using $CHCl_3$ as eluent. Compound **6** was obtained as a white solid. Yield: (620 mg, 52%). Anal. Calc. for $C_7H_{23}B_9S$ (%): C, 35.56; H, 9.73; S, 13.54. Found: C, 35.05; H, 9.56; S, 13.06. IR ν: 2974, 2925, 2868 (C–H); 2546. ^{1}H-NMR: δ −1.07 (br quadruplet, 1H, ^1J(B, H) = 80, B–H–B); 1.48 (dd, 6H, $^3J(H_a, H) = 7.4$, $^3J(H_b, H) = 7.7$, CH_3); 1.49 (s, 3H, CH_3); 2.10 (br s, 1H, Cc–H); 2.89 (dq, 2H, $^2J(H_a, H_b) = 13.2$, $^3J(H_a, H) = 7.4$, S–CH_a, S–$CH_{a'}$ (SCH_2)); 3.02 (dq, 2H, $^2J(H_b, H_a) = 12.9$, $^3J(H_b, H) = 7.7$, S–CH_b, S–$CH_{b'}$ (SCH_2)). ^{11}B-NMR: δ −10.7 (d, 1B, ^1J(B, H) = 141); −11.2 (d, 1B, ^1J(B, H) = 142); −12.4 (d, 1B, ^1J(B, H) = 161); −16.1 (d, 2B, ^1J(B, H) = 149), −17.2 (d, 1B, ^1J(B, H) = 138); −20.3 (d, 1B, ^1J(B, H) = 155); −27.0 (d, 1B, ^1J(B, H) = 80); −36.0 (d, 1B, ^1J(B, H) = 143). ^{13}C{^{1}H}-NMR: δ 11.9 (s, CH_3); 25.4 (s, CH_3); 35.0 (s, S–CH_2); 53.3 (br s, C_c); 59.8 (br s, C_c).

3.8.1. Thermolysis

The charge-compensated ligands **1**–**3** (50 mg) were dissolved in 10 ml of aromatic solvent (mesitylene or xylene). The solutions were refluxed under dinitrogen for several hours depending on the ligand. Samples were taken at various time intervals and the thermolysis was followed by ^{11}B-NMR spectroscopy. Estimations of the relative concentrations of species were made from all peak areas (see Tables 3 and 4).

3.9. X-Ray Studies of 1 and 3

Single-crystal data collections for **1** and **3** were performed at ambient temperature on a Rigaku AFC5S diffractometer using graphite monochromatized Mo–Kα radiation. The unit cell parameters were determined by least-squares refinement of 25 carefully centred reflections. The structures were solved by direct methods and refined by full-matrix least-squares on F^2 techniques using the SHELX-97 program package. [9] For **1**, all non-hydrogen atoms were refined with anisotropic displacement parameters. For **3**, $S(CH_2)_4$ group is disordered assuming two orientations with site occupation parameters 0.773(7) (conformation **A**) and 0.227(7) (conformation **B**). Non-hydrogen atoms of the carborane cage and S1a and S1b were refined with anisotropic displacement parameters and the disordered carbon atoms with isotropic displacement parameters. Constraint U(S1a) = U(S1b) and DFIX restraints were used for the disordered part of the molecule in the refinement.

Table 5
Crystallographic data for compounds **1** and **3**

	1	3
Empirical formula	$C_4H_{17}B_9S$	$C_6H_{19}B_9S$
Formula weight	194.53	220.56
Wavelength (Å)	0.71069	0.71069
Crystal system	Orthorhombic	Orthorhombic
Space group	*Pbcn* (no. 60)	*Pbca* (no. 61)
Unit cell dimensions		
a (Å)	10.9985(15)	14.186(3)
b (Å)	14.1274(16)	14.843(2)
c (Å)	14.8928(15)	12.2443(16)
V (Å^3)	2314.0(4)	2578.2(7)
Z	8	8
D_{calc} (g cm^{-3})	1.117	1.136
μ (cm^{-1})	2.24	2.09
Number of unique reflections	2042	2269
Number of parameters	145	160
$R_1(F_o)$ [a] $[I > 2\sigma(I)]$	0.0439	0.0599
$wR_2(F_o^2)$ [b] $[I > 2\sigma(I)]$	0.1072	0.1440
Goodness-of-fit on F^2	1.017	1.034
Largest differential peak and hole (e/Å^{-3})	0.228 and −0.194	0.335 and −0.262

[a] $R_1 = \Sigma||F_o| - |F_c||/\Sigma|F_o|$.
[b] $wR_2 = [\Sigma\, w(|F_o^2| - |F_c^2|)^2/\Sigma\, w|F_o^2|^2]^{1/2}$.

For both compounds, hydrogen atoms were included in the calculations at fixed distances from their host atoms and treated as riding atoms using the SHELX-97 default parameters or refined isotropically (hydrogen atoms at C7, C8, B9, B10 and B11). Crystallographic data are listed in Table 5.

4. Supplementary material

Crystallographic data (excluding structure factors) for the structures reported in this paper have been deposited with the Cambridge Crystallographic Data Centre, CCDC nos. 168130 and 168131 for compounds **1** and **3**. Copies of this information may be obtained free of charge from The Director, CCDC, 12 Union Road, Cambridge CB2 1EZ, UK (Fax: +44-1223-336033; e-mail: deposit@ccdc.cam.ac.uk or www: http://www.ccdc.cam.ac.uk).

Acknowledgements

This work was supported by CICYT (Project MAT98-0921 and a doctoral grant (O.T.) joined to the project), Generalitat de Catalunya (2000SGR/00108) and Academy of Finland (project 41519, RK).

References

[1] (a) M.F. Hawthorne, D.C. Young, P.A. Wegner, J. Am. Chem. Soc. 87 (1965) 1818;
(b) M.F. Hawthorne, R.L. Pilling, J. Am. Chem. Soc. 87 (1965) 3987;
(c) M.F. Hawthorne, D.C. Young, T.D. Andrews, D.V. Howe, R.L. Pilling, A.D. Pitts, M. Reinties, L.F. Warren, Jr., P.A. Wegner, J. Am. Chem. Soc. 90 (1968) 879;
(d) M. Green, J.L. Spencer, F.G.A. Stone, J. Chem. Soc. Dalton Trans. (1975) 179;
(e) F.G.A. Stone, J. Organomet. Chem. 100 (1975) 257;
(f) J. Cowie, E.J.M. Hamilton, J.C.V. Laurie, A.J. Welch, J. Organomet. Chem. 394 (1990) 1;
(g) C.E. Housecroft, in: E.W. Abel, F.G.A. Stone (Eds.), Specialist Periodical Reports in Organometallic Chemistry, Royal Society of Chemistry, London, 1991;
(h) S.A. Brew, F.G.A. Stone, Adv. Organomet. Chem. 35 (1993) 135;
(i) R.N. Grimes, in: E. Able, F.G.A. Stone, G. Wilkinson (Eds.), Comprehensive Organometallic Chemistry II, vol. 1 (chapter 9), Pergamon Press, Oxford, England, 1995, p. 373;
(j) S.A. Anderson, D.F. Mullica, E.L. Sappenfield, F.G.A. Stone, Organometallics 14 (1995) 3516;
(k) A.K. Saxena, J.A. Maguire, N.S. Hosmane, Chem. Rev. 97 (1997) 2421.
[2] (a) F.N. Tebbe, P.M. Garret, M.F. Hawthorne, J. Am. Chem. Soc. 90 (1968) 869;
(b) J. Plesek, Z. Janousek, S. Hermánek, Collect. Czech. Chem. Commun. 43 (1978) 2862;
(c) H.C. Kang, S.S. Lee, C.B. Knobler, M.F. Hawthorne, Inorg. Chem. 30 (1991) 2024;
(d) J. Plesek, T. Jelínek, F. Mares, S. Hermánek, Collect. Czech. Chem. Commun. 58 (1993) 1534;
(e) G.M. Rosair, A.J. Welch, A.S. Weller, S.K. Zahn, J. Organomet. Chem. 536 (1997) 299;
(f) S. Dunn, R.M. Garrioch, G.M. Rosair, L. Smith, J.A. Welch, Collect. Czech. Chem. Commun. 64 (1999) 1013.
[3] J. Plesek, Z. Janousek, S. Hermánek, Inorg. Synt. 22 (1983) 239.
[4] D.C. Young, D.V. Howe, M.F. Hawthorne, J. Am. Chem. Soc. 91 (1969) 859.
[5] (a) D.A. Owen, M.F. Hawthorne, J. Am. Chem. Soc. 91 (1969) 6002;
(b) V. Chowdhry, W.R. Pretzer, D.N. Rai, R.W. Rudolph, J. Am. Chem. Soc. 95 (1973) 4560.
[6] J. Cowie, E.J.M. Hamilton, J.C.V. Laurie, A.J. Welch, Acta Crystallogr. C44 (1988) 1648.
[7] (a) L.I. Zakharkin, G.G. Zhigareva, V.A. Antonovich, A.I. Yanovskii, Yu.T. Struchkov, Izv. Akad. Nauk SSSR. Ser. Khim. (1984) 1672;
(b) L.I. Zakharkin, G.G. Zhigareva, V.A. Antonovich, A.I. Yanovskii, Zh. Obsch. Khim. 56 (1986) 2066;
(c) B. Stibr, Chem. Rev. 92 (1992) 243.
[8] J. Plesek, S. Hermanek, B. Stibr, Inorg. Synth. 22 (1983) 231.
[9] G.M. Sheldrick, SHELX-97, Universität Göttingen, 1997.

Pergamon

Tetrahedron Letters 43 (2002) 983–987

TETRAHEDRON LETTERS

Olefin cyclopropanation catalysed by half-sandwich ruthenium complexes

Oscar Tutusaus,[a] Sébastien Delfosse,[b] Albert Demonceau,[b,*] Alfred F. Noels,[b] Rosario Núñez,[a] Clara Viñas[a,*] and Francesc Teixidor[a]

[a]*Institut de Ciència de Materials de Barcelona, CSIC, Campus de Bellaterra, Cerdanyola, 08193 Barcelona, Spain*
[b]*Laboratory of Macromolecular Chemistry and Organic Catalysis, University of Liège, Sart-Tilman (B.6a), B-4000 Liège, Belgium*

Received 23 October 2001; accepted 29 November 2001

Abstract—Ruthenium complexes of the type $[RuX(Cp')(PPh_3)_2]$ (X = Cl and H; Cp' = Cp, Cp*, indenyl, and carboranyl) efficiently catalyse olefin cyclopropanation with diazoesters, and the *cis/trans* stereoselectivity of the resulting cyclopropanes strongly depends on the Cp' ligand. With $[RuCl(Cp^*)(PAr_3)_2]$ complexes, cyclopropanation competes with the formal carbene insertion into C–H vinyl bonds of styrene, whereas ring-opening metathesis polymerisation takes place with norbornene, lending support to the formation of ruthenium–carbene and ruthenacyclobutanes as intermediates in these reactions. © 2002 Elsevier Science Ltd. All rights reserved.

In recent decades there has been an exponential increase in the use of transition metals in organic synthesis. Among the different types of transition-metal-based reagents described, carbene complexes are among the most versatile.[1] The applications of carbene complexes include both their use as catalysts for a number of important synthetic transformations[2] and their utilisation as stoichiometric reagents.[3] In the period between the discovery in the late 1950s that copper catalysed the addition of diazo compounds to olefins to yield cyclopropanes and the introduction of chiral catalysts for asymmetric cyclopropanation,[4] a wide variety of useful transition-metal-based catalysts has been discovered. Nowadays, rhodium carboxylates, discovered by Noels and Hubert in the early 1970s,[5] play a prominent role in carbene chemistry, and display some of the highest efficiency and versatility.

Ruthenium has been introduced recently as a much cheaper alternative to rhodium,[6] and quite interesting results have been reported in the literature.[7] Until now, however, limitations associated with most ruthenium complexes include failure to cyclopropanate inactivated olefins, and quite low turnover numbers. In addition, the factors governing catalyst activity and the mechanism by which ruthenium catalysts perform olefin cyclopropanation are not known.[8] Investigations were undertaken to address both of these topics in the following way: by varying the ligand sphere around the ruthenium catalyst, we wished to determine how the electronic and steric properties of the ligands affect catalyst activity. Ruthenium complexes of the type $[RuX(Cp')(PPh_3)_2]$ (X = Cl, H; Cp' = Cp, Cp*, indenyl, and carboranyl) (**1–4**, Scheme 1) were chosen as potential catalysts for two reasons: (1) upon Cp' ligand substitution, it is expected to modify the electronic contributions in these systems. The higher electron donating ability of Cp* compared to Cp is well-established,[9] and the capacity of carboranyl ligands ($[C_2B_9H_{11}]^{2-}$) to stabilise uncommon and high oxidation states of the metals as well.[10] (2) On the other hand, Cp' substitution also results in changing the steric properties of the ligands, which are expressed by the cone angle. In this way, Cp* is obviously bulkier than Cp and, most probably, than the carboranyl ligand $[C_2B_9H_{11}]^{2-}$,[11a,b] although the relative size of the latter compared to Cp and Cp* is still a question under debate.[11c,d] The indenyl ligand poses a more complex problem since it is known to undergo a facile metal ring slippage from η^5- to η^3-coordination, leading to the creation of a vacant coordination site on the metal to host an entering ligand or substrate.[12]

Keywords: cyclopropanation; diazo compounds; metathesis; olefins; ruthenium and compounds.

* Corresponding authors. Fax: 32-(0)4 366 3497 (A.D.); fax: 34-(0)93/580 57 29 (C.V.); e-mail: a.demonceau@ulg.ac.be; clara@icmab.es

0040-4039/02/$ - see front matter © 2002 Elsevier Science Ltd. All rights reserved.
PII: S0040-4039(01)02292-4

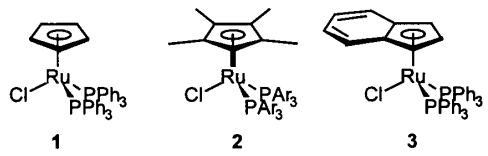

1 2 3

(a) Ar = C_6H_5
(b) Ar = p-C_6H_4-OCH_3
(c) Ar = p-C_6H_4-CF_3

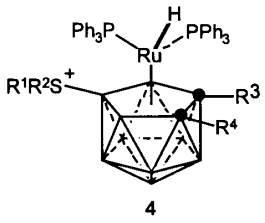

4

(a) $R^1 = R^2 = CH_3$, $R^3 = R^4 = H$
(b) R^1-$R^2 = (CH_2)_4$, $R^3 = R^4 = H$
(c) $R^1 = R^2 = CH_3$, $R^3 = CH_3$, $R^4 = H$

Scheme 1.

In this paper, we report that ruthenium complexes of the type $[RuX(Cp')(PAr_3)_2]$ (X = Cl, H; Cp' = Cp,[13] Cp*,[14] indenyl, and carboranyl[15]) efficiently catalyse the cyclopropanation of styrenics with diazoesters.

To determine the relative activities and stereoselectivities of ruthenium catalysts **1–4**, the cyclopropanation of styrene with ethyl diazoacetate was measured under a standard set of conditions (Scheme 2, R = Ph). The results are summarised in Table 1. The half-sandwich ruthenium complex, $[RuCl(Cp)(PPh_3)_2]$ (**1**), proved to be an effective catalyst for cyclopropanation of styrene. Cyclopropane products were obtained in high yield and with predominantly *cis* stereoselectivity. To examine the influence of the Cp' ligand toward catalyst activity, the half-sandwich ruthenium compounds **2–4** were then employed. Compared to **1**, complexes **2–4** led to the reversed stereoselectivity, with the *trans* isomer as the main product. On the other hand, ruthenacarboranes **4** gave rise to cyclopropanation yields similar to that of **1**. Noteworthy, with the related complexes, $[RuCl(Cp^*)(PPh_3)_2]$ (**2a**) and $[RuCl(Ind)(PPh_3)_2]$ (**3**), the reaction of ethyl diazoacetate with styrene proceeded smoothly. Catalysts **2a** and **3** showed a lower catalytic activity (around 60% cyclopropanation yield); however, carbene insertion into the vinylic C–H bonds was also observed to some extent. Upon monitoring by gas chromatography the reaction of styrene and ethyl diazoacetate catalysed by $[RuCl(Cp^*)(PPh_3)_2]$, it was determined that in addition to forming the cyclopropanes, the C–H insertion products **5** and **6** (Scheme 3) appear initially as well.

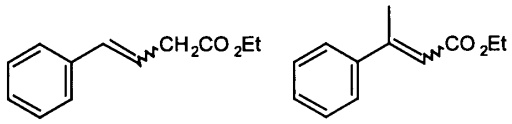

5 6

Scheme 3.

In addition, it was observed that the product distribution does not change over the course of the reaction, indicating that the products **5** and **6** are not formed by ruthenium-assisted opening of the cyclopropanes. For styrene, the combined cyclopropanation and C–H insertion products were isolated in 97% yield, and the product distribution was determined to be 57:22:18, respectively. Noteworthy, formation of C–H insertion products is distinctive of the [Ru–Cp*] fragment, and is independent of the phosphine used: [RuCl(Cp*)] complexes with isosteric *para*-substituted triarylphosphines differing only by their electronic contributions (PPh_3 (**2a**), $P(p\text{-}C_6H_4\text{-}OCH_3)_3$ (**2b**), and $P(p\text{-}C_6H_4\text{-}CF_3)_3$ (**2c**)) gave the same reactivity pattern.

Having established that complexes **1** and **4** show the best catalytic performance for the cyclopropanation of styrene, we then investigated the reaction of ethyl diazoacetate with different styrene derivatives, 1-octene and cyclooctene as well. The reactions were carried out at 40°C, a temperature which, while being fairly moderate, allows for olefin cyclopropanation to be accomplished efficiently (Fig. 1). The results of the cycloaddition reactions are displayed in Table 2. In line with the previous data obtained with styrene as starting material, the reactions of ethyl diazoacetate with styrenics afforded the corresponding cyclopropanes in good yields, with predominantly *cis* stereoselectivity

Table 1. Ruthenium-catalysed cyclopropanation of styrene by ethyl diazoacetate[a]

	Cyclopropanation	
Complex	Yield (%)[b]	*cis*/*trans* ratio
1	85	1.85
2a	57	0.17
2b	59	0.25
2c	61	0.30
3	68	0.48
4a	85	0.48
4b	86	0.52
4c	88	0.52

[a] *Reaction conditions*: complex, 0.005 mmol; styrene, 2 mL; ethyl diazoacetate, 1 mmol diluted in 1 mL of styrene; addition time, 4 h; 40°C.
[b] Based on ethyl diazoacetate.

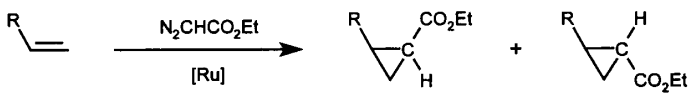

Scheme 2.

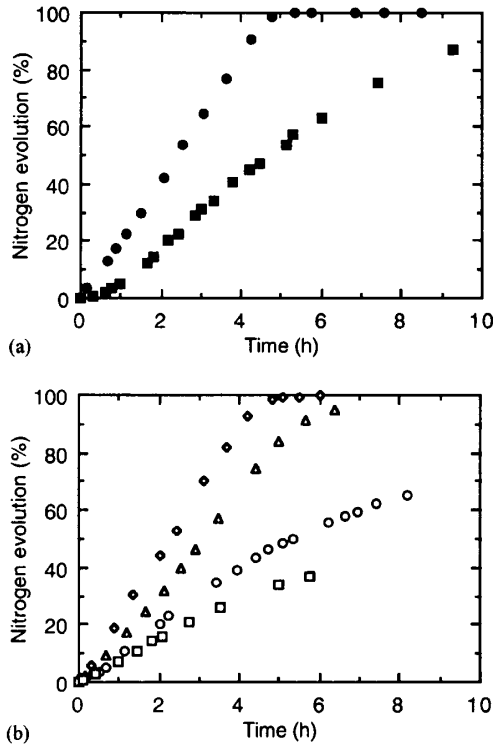

Figure 1. Influence of the temperature on the decomposition rate of ethyl diazoacetate in styrene in the presence of complexes **1** (rt (■), and 40°C (●)), and **4a** (rt (□), 40°C (○), 60°C (△) and 80°C (◇). Reaction conditions same as in Table 1.

with catalyst **1**, and *trans* stereoselectivity with complex **4a**. By contrast, non activated olefins (1-octene and cyclooctene) were much less reactive, giving mainly dimethyl maleate and only minor cyclopropanation products. Apparently, electron-rich olefins show a higher reactivity toward the intermediate carbene species, and thus carbene dimerisation can be suppressed.

$[RuCl(Cp')(PAr_3)_2]$ are 18-electron complexes, and it is generally agreed that the catalytic activity of this class of ruthenium complexes depends on the relative facility of dissociation of one phosphine.[13,16] It is therefore reasonable to assume that the initial stage of the catalytic cyclopropanation of olefins implies the generation of the carbene intermediate $[RuCl(=CHCO_2Et)(Cp')(PAr_3)]$, by reaction of the diazo compound with the 16-electron complex $[RuCl(Cp')(PAr_3)]$ formed by displacement of one phosphine ligand.[13] With this in mind, the formation of the cyclopropanes could then occur though the transfer of the carbene fragment onto a non coordinated olefin. This hypothesis, however, does not account for the formation of product **6**. According to the literature,[8,13,17] the formation of **6** (and **5** as well) would result rather from the rearrangement (likely via an η^3-allylhydrido intermediate) of a metallacyclobutane, a key intermediate in olefin metathesis which is in equilibrium with a metal–carbene–olefin complex. If we postulate the intermediacy of ruthenacyclobutanes in the formation of compounds **5** and **6**, metallacyclobutanes should be detectable by their propensity to initiate the formation of polymers from a suitable cyclic olefin. In order to test this hypothesis, we tested complexes **1**–**4** in the ring-opening metathesis polymerisation (ROMP) of norbornene (Scheme 4). Moderate amounts of polynorbornenes (up to 63% yields) were formed, essentially with catalysts **2** and **3** when activated by reaction with trimethylsilyldiazomethane, which is usually superior to diazoesters for initiating metathesis.[18] Most gratifyingly, we also noted that the most efficient catalysts for olefin homologation were also the most active ones for ROMP (Table 3), therefore supporting the assumption of the intermediacy of a ruthenacyclobutane in the homologation reaction. A speculative catalytic cycle is presented on Scheme 5.

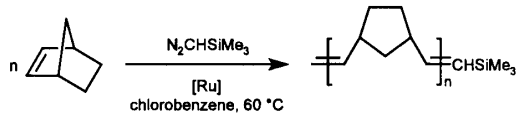

Scheme 4.

Table 2. Ruthenium-catalysed cyclopropanation of various olefins by ethyl diazoacetate[a]

Olefin	Complex **1** Cyclopropanation		Complex **4a** Cyclopropanation	
	Yield (%)[b]	*cis*/*trans* ratio	Yield (%)[b]	*cis*/*trans* ratio
Styrene	85	1.85	85	0.48
4-Methylstyrene	87	1.17	86	0.49
4-*tert*-Butylstyrene	82	1.01	81	0.59
4-Methoxystyrene	89	1.27	84	0.68
4-Chlorostyrene	87	1.45	79	0.62
α-Methylstyrene	82	1.63	84	1.13
1-Octene	5	0.39	39	0.60
Cyclooctene	16	1.33[c]	15	0.60[c]

[a] Same as in Table 1.
[b] Same as in Table 1.
[c] *endo*/*exo* ratio.

Table 3. Ring-opening metathesis polymerisation of norbornene catalysed by complexes **1–4**[a]

Complex	Polymer yield (%)	M_n[b]	M_w/M_n[b]	σ_c[c]
1	1	–	–	0.38
2a	26	–	–	0.54
2b	19	–	–	0.44
2c	63	–	–	0.36
3	55	35 500	7.7	0.54
4a	7	33 500	10.6	0.66
4b	1	39 000	11.5	–
4c	2	39 500	10.7	0.36

[a] *Reaction conditions*: 0.0075 mmol of catalyst and 0.5 g of norbornene were dissolved under nitrogen in 30 mL of purified chlorobenzene. The resulting solution was heated to 60°C over 20 min, and 0.1 mmol of trimethylsilyldiazomethane diluted in 1 mL of chlorobenzene was then added to the reaction mixture via a syringe. The reaction mixture was kept at 60°C for 5 h, then cooled to room temperature, and precipitated in 700 mL of technical methanol.

[b] Determined by GPC, using polystyrene standards.

[c] Fraction of *cis* units, determined by ^1H and ^{13}C NMR.

The formation of ruthenacyclobutanes infers that the carbene and the olefin are both coordinated to the metal centre, and hence the presence of two *cis* vacancies resulting either from the displacement of two phosphine ligands from the $[RuCl(Cp')(PAr_3)_2]$ complexes or the release of only one phosphine and metal ring-slippage of indenyl in $[RuCl(Ind)(PPh_3)_2]$. The formation of ruthenacyclobutanes also infers the generation of Ru^{IV} species. Not surprisingly, the Cp* and indenyl ligands are known to display electron-releasing properties that are much more pronounced than those of Cp.[19] Accordingly, the [RuCl(Cp')] moiety (Cp'=Cp* and Ind) should stabilise the Ru^{IV}–cyclobutane more reliably than [RuClCp], favouring therefore a metathetical reaction pathway.

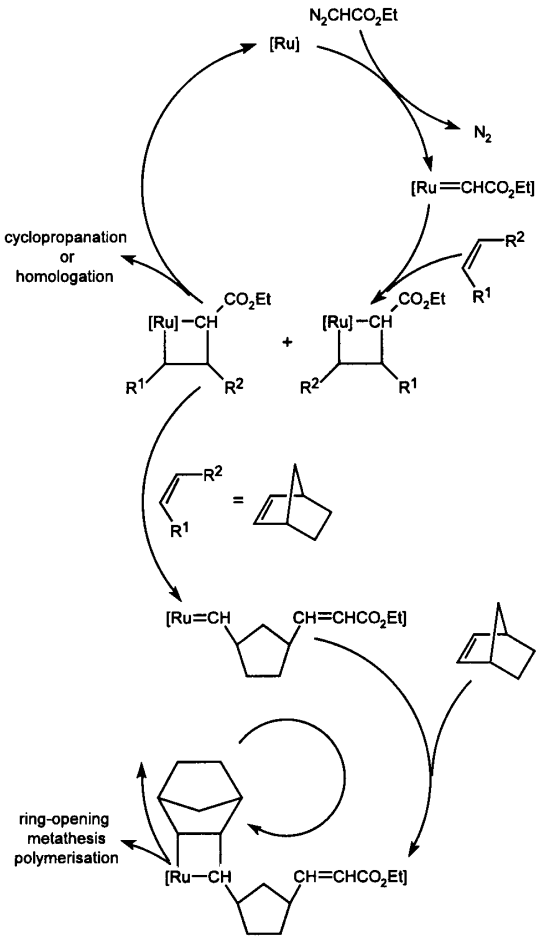

Scheme 5.

The intermediacy of ruthenacyclobutanes in the homologation reaction of olefins remains, however, questionable, and observing olefin metathesis does not infer that homologation takes place via the same ruthenacyclobutane intermediate. Alternative mechanisms could be proposed to account for olefin homologation. Nevertheless, it is well-known in organometallic chemistry that ruthenacyclobutanes are very unstable species, and only very few have been synthesised and fully characterised.[20] In olefin metathesis, a reaction in which the intermediacy of a metallacyclobutane seems to be no doubt, ruthenacyclobutanes have never been detected despite numerous efforts world-wide.[21] In addition, theoretical studies, including molecular dynamics simulations,[22] revealed the formation of a ruthenacyclobutane intermediate, but in a very high-energy state. In the present case, since the activity of the ruthenium catalysts for olefin homologation parallels pretty well that for olefin metathesis, the involvement of a common ruthenacyclobutane intermediate for both reactions is quite plausible, though speculative. However, due to the transient nature of ruthenacyclobutanes, a clear spectroscopic evidence for their intermediacy in the homologation reaction seems to be out of reach nowadays.

In conclusion, we have shown that $[RuCl(Cp)(PPh_3)_2]$ (**1**) and their carboranyl derivatives (**4**) are highly efficient catalyst precursors for promoting olefin cyclopropanation under mild conditions, with **1** exhibiting a high *cis* stereoselectivity and **4** a significant preference for the *trans* isomers. In addition to forming cyclopropanes, $[RuCl(Cp^*)(PAr_3)_2]$ (**2**) also catalyses the insertion of carbenes into vinylic C–H bonds likely via a ruthenacyclobutane intermediate. A detailed understanding of the reaction mechanism must await further study, and improvements with this family of ruthenium(II) complexes through modification of the stereoelectronic parameters of the ligands are now under investigation.

Acknowledgements

This work was financially supported by a grant-in-aid (O.T.) joined to the project MAT98-0921 from CICYT (Spain). Part of this work has also been carried out in the framework of the COST D17/006/00 and TMR-HPRN CT 2000-10 'Polycat' programmes. The Belgian team is also grateful to the 'Fonds National de la

Recherche Scientifique' (F.N.R.S.), Brussels, for the purchase of major instrumentation.

References

1. Zaragoza Dörwald, F. *Metal Carbenes in Organic Synthesis*; Wiley-VCH: Weinheim, 1999.
2. (a) Maas, G. *Top. Curr. Chem.* **1987**, *137*, 75–253; (b) Ye, T.; McKervey, M. A. *Chem. Rev.* **1994**, *94*, 1091–1160; (c) Noels, A. F.; Demonceau, A. In *Applied Homogeneous Catalysis with Organometallic Compounds*; Cornils, B.; Herrmann, W. A., Eds.; VCH: Weinheim, 1996; Vol. 2: Developments, pp. 733–747.
3. (a) Dötz, K. H.; Tomuschat, P. *Chem. Soc. Rev.* **1999**, *28*, 187–198; (b) Herndon, J. W. *Tetrahedron* **2000**, *56*, 1257–1280; (c) Barluenga, J.; Fañanás, F. J. *Tetrahedron* **2000**, *56*, 4597–4628; (d) Sierra, M. A. *Chem. Rev.* **2000**, *100*, 3591–3637.
4. (a) Nozaki, H.; Moriuti, S.; Takaya, H.; Noyori, R. *Tetrahedron Lett.* **1966**, *7*, 5239–5244; (b) Doyle, M. P.; Protopopova, M. N. *Tetrahedron* **1998**, *54*, 7919–7946; (c) Doyle, M. P.; Forbes, D. C. *Chem. Rev.* **1998**, *98*, 911–935.
5. (a) Paulissen, R.; Reimlinger, H.; Hayez, E.; Hubert, A. J.; Teyssié, P. *Tetrahedron Lett.* **1973**, *14*, 2233–2236; (b) Hubert, A. J.; Noels, A. F.; Anciaux, A. J.; Teyssié, P. *Synthesis* **1976**, 600–602.
6. (a) Demonceau, A.; Noels, A. F.; Saive, E.; Hubert, A. J. *J. Mol. Catal.* **1992**, *76*, 123–132; (b) Demonceau, A.; Saive, E.; de Froidmont, Y.; Noels, A. F.; Hubert, A. J.; Chizhevsky, I. T.; Lobanova, I. A.; Bregadze, V. I. *Tetrahedron Lett.* **1992**, *33*, 2009–2012; (c) Demonceau, A.; Abreu Dias, E.; Lemoine, C. A.; Stumpf, A. W.; Noels, A. F.; Pietraszuk, C.; Gulinski, J.; Marciniec, B. *Tetrahedron Lett.* **1995**, *36*, 3519–3522; (d) Demonceau, A.; Lemoine, C. A.; Noels, A. F.; Chizhevsky, I. T.; Sorokin, P. V. *Tetrahedron Lett.* **1995**, *36*, 8419–8422; (e) Demonceau, A.; Simal, F.; Noels, A. F.; Viñas, C.; Nuñez, R.; Teixidor, F. *Tetrahedron Lett.* **1997**, *38*, 4079–4082; (f) Simal, F.; Demonceau, A.; Noels, A. F. *Tetrahedron Lett.* **1998**, *39*, 3493–3496; (g) Simal, F.; Jan, D.; Demonceau, A.; Noels, A. F. *Tetrahedron Lett.* **1999**, *40*, 1653–1656; (h) Teixidor, F.; Núñez, R.; Flores, M. A.; Demonceau, A.; Viñas, C. *J. Organomet. Chem.* **2000**, *614–615*, 48–56.
7. (a) Bergbreiter, D. E.; Morvant, M.; Chen, B. *Tetrahedron Lett.* **1991**, *32*, 2731–2734; (b) Maas, G.; Werle, T.; Alt, M.; Mayer, D. *Tetrahedron* **1993**, *49*, 881–888; (c) Doyle, M. P.; Peterson, C. S.; Zhou, Q.-L.; Nishiyama, H. *J. Chem. Soc., Chem. Commun.* **1997**, 211–212; (d) Davies, I. W.; Gerena, L.; Cai, D.; Larsen, R. D.; Verhoeven, T. R.; Reider, P. J. *Tetrahedron Lett.* **1997**, *38*, 1145–1148; (e) Frauenkron, M.; Berkessel, A. *Tetrahedron Lett.* **1997**, *38*, 7175–7176; (f) Lo, W.-C.; Che, C.-M.; Cheng, K.-F.; Mak, T. C. W. *J. Chem. Soc., Chem. Commun.* **1997**, 1205–1206 and 2249; (g) Galardon, E.; Roué, S.; Le Maux, P.; Simonneaux, G. *Tetrahedron Lett.* **1998**, *39*, 2333–2334; (h) Gross, Z.; Galili, N.; Simkhovich, L. *Tetrahedron Lett.* **1999**, *40*, 1571–1574; (i) Song, J.-H.; Cho, D.-J.; Jeon, S.-J.; Kim, Y.-H.; Kim, T.-J.; Jeong, J. H. *Inorg. Chem.* **1999**, *38*, 893–896; (j) Saha, B.; Uchida, T.; Katsuki, T. *Synlett* **2001**, 114–116; (k) Zheng, Z.; Yao, X.; Li, C.; Chen, H.; Hu, X. *Tetrahedron Lett.* **2001**, *42*, 2847–2849 and references cited therein.
8. (a) Noels, A. F.; Demonceau, A. *J. Phys. Org. Chem.* **1998**, *11*, 602–609; (b) Simal, F.; Demonceau, A.; Noels, A. F.; Knowles, D. R. T.; O'Leary, S.; Maitlis, P. M.; Gusev, O. V. *J. Organomet. Chem.* **1998**, *558*, 163–170.
9. Serron, S. A.; Luo, L.; Li, C.; Cucullu, M. E.; Stevens, E. D.; Nolan, S. P. *Organometallics* **1995**, *14*, 5290–5297.
10. Saxena, A. K.; Hosmane, N. S. *Chem. Rev.* **1993**, *93*, 1081–1124.
11. (a) Hawthorne, M. F.; Young, D. C.; Andrews, T. D.; Howe, D. V.; Pilling, R. L.; Pitts, A. D.; Reintjes, M.; Warren, L. F., Jr.; Wegner, P. A. *J. Am. Chem. Soc.* **1968**, *90*, 879–896; (b) White, D.; Coville, N. J. *Adv. Organomet. Chem.* **1994**, *36*, 95–158; (c) Hanusa, T. P. *Polyhedron* **1982**, *1*, 663–665; (d) Crowther, D. J.; Baenziger, N. C.; Jordan, R. F. *J. Am. Chem. Soc.* **1991**, *113*, 1455–1457.
12. Rerek, M. E.; Ji, L.-N.; Basolo, F. *J. Chem. Soc., Chem. Commun.* **1983**, 1208–1209.
13. Baratta, W.; Herrmann, W. A.; Kratzer, R. M.; Rigo, P. *Organometallics* **2000**, *19*, 3664–3669.
14. Fagan, P. J.; Mahoney, W. S.; Calabrese, J. C.; Williams, I. D. *Organometallics* **1990**, *9*, 1843–1852.
15. Tutusaus, O.; Núñez, R.; Viñas, C.; Teixidor, F., to be published.
16. (a) Del Zotto, A.; Baratta, W.; Rigo, P. *J. Chem. Soc., Perkin Trans. 1* **1999**, 3079–3081; (b) Simal, F.; Wlodarczak, L.; Demonceau, A.; Noels, A. F. *Tetrahedron Lett.* **2000**, *41*, 6071–6074; (c) Simal, F.; Wlodarczak, L.; Demonceau, A.; Noels, A. F. *Eur. J. Org. Chem.* **2001**, 2689–2695.
17. (a) Werner, H.; Möhring, U. *J. Organomet. Chem.* **1994**, *475*, 277–282; (b) Werner, H.; Bosch, M.; Schneider, M. E.; Hahn, C.; Kukla, F.; Manger, M.; Windmüller, B.; Weberndörfer, B.; Laubender, M. *J. Chem. Soc., Dalton Trans. 1* **1998**, 3549–3558.
18. Demonceau, A.; Stumpf, A. W.; Saive, E.; Noels, A. F. *Macromolecules* **1997**, *30*, 3127–3136.
19. Gamasa, M. P.; Gimeno, J.; Gonzalez-Bernardo, C.; Martin-Vaca, B. M.; Monti, D.; Bassetti, M. *Organometallics* **1996**, *15*, 302–308.
20. (a) Jennings, P. W.; Johnson, L. L. *Chem. Rev.* **1994**, *94*, 2241–2290; (b) Demonceau, A.; Jan, D.; Noels, A. F.; Simal, F. In *Education in Advanced Chemistry*; Marciniec, B., Ed. Mechanistic aspects of molecular catalysis. Wydawnictwo Poznanskie: Poznan-Wroclaw, 1999; Vol. 6, pp. 49–70.
21. (a) Tallarico, J. A.; Bonitatebus, P. J., Jr.; Snapper, M. L. *J. Am. Chem. Soc.* **1997**, *119*, 7157–7158; (b) Pietraszuk, C.; Marciniec, B.; Fischer, H. *Organometallics* **2000**, *19*, 913–917; (c) Pietraszuk, C.; Fischer, H. *Chem. Commun.* **2000**, 2463–2464; (d) Trnka, T. M.; Grubbs, R. H. *Acc. Chem. Res.* **2001**, *34*, 18–29; (e) Demonceau, A.; Noels, A. F., unpublished results.
22. Aagaard, O. M.; Meier, R. J.; Buda, F. *J. Am. Chem. Soc.* **1998**, *120*, 7174–7182.

ELSEVIER

Inorganic Chemistry Communications 5 (2002) 941–945

INORGANIC CHEMISTRY COMMUNICATIONS

www.elsevier.com/locate/inoche

Half-sandwich ruthenium complexes for the controlled radical polymerisation of vinyl monomers

Oscar Tutusaus [a,1], Sébastien Delfosse [b], François Simal [b,2], Albert Demonceau [b,*], Alfred F. Noels [b], Rosario Núñez [a], Clara Viñas [a], Francesc Teixidor [a,3]

[a] *Institut de Ciència de Materials, CSIC-UAB, Campus de Bellaterra, Cerdanyola, 08193 Barcelona, Spain*
[b] *Laboratory of Macromolecular Chemistry and Organic Catalysis, University of Liège, Sart-Tilman (B.6a), B-4000 Liège, Belgium*

Received 26 July 2002; accepted 23 August 2002

Abstract

Ruthenium complexes of the type $[RuX(Cp^{\#})(PPh_3)_2]$ (X = Cl and H; $Cp^{\#}$ = Cp, Cp*, indenyl, and carboranyl) catalyse the radical polymerisation of styrene and *n*-butyl acrylate, and both the catalyst activity and the degree of control of the polymerisation strongly depend on the $Cp^{\#}$ ligand and the monomer.

Keywords: Homogeneous catalysis; Olefins; Polymerisations; Radical reactions; Ruthenium and compounds

It was in 1995 that Sawamoto and coworkers [1] and Matyjaszewski and Wang [2] independently reported their seminal papers on atom transfer radical polymerisation (ATRP) [3a,3b]. This process takes advantage of the redox properties of transition metals, and is based on a dynamic equilibration between active propagating radicals and dormant species. This equilibrium is established through the reversible transition metal-catalysed homolytic cleavage of the covalent carbon–halogen bond in the dormant species (Scheme 1).

Catalytic engineering at the metal centre aims to shift this equilibrium toward the dormant species. Thus, the concentration of propagating radicals remains low thorough the whole polymerisation process and a high degree of control ensues, allowing not only the synthesis of polymers of predictable molecular weights and low polydispersities, but also the preparation of novel, functionalised, block copolymers amenable to further transformations.

Among the numerous catalytic systems developed for ATRP, ruthenium play a prominent role [1,3a,4a,4b]. We recently reported on the exceptional efficiency and versatility of new catalysts based on $[RuCl_2(p\text{-cymene})(PR_3)]$ [5] (*p*-cymene is 4-isopropyltoluene) and $[RuCl_2(=CHPh)(L)(L')]$ [6] (L, L′ are PR_3 and *N*-heterocyclic carbenes) for promoting the ATRP of vinyl monomers. Later on, Sawamoto and coworkers [7] and Simal et al. [8] independently discovered that half-sandwich ruthenium complexes **1–3** were efficient and markedly active catalysts for the controlled radical polymerisation of vinyl monomers and the Kharasch addition as well.

Nowadays, the factors governing catalyst activity and the mechanism by which half-sandwich ruthenium catalysts perform radical reactions are not known. Investigations were undertaken to address both of these topics in the following way: by varying the ligand sphere around the ruthenium catalyst, we wished to determine how the electronic and steric properties of the ligands affect catalyst activity. Ruthenium complexes **1–3** and ruthenacarboranes [9] **4** (Scheme 2) were compared for two reasons: (1) the cyclopentadienyl anion (Cp), its derivatives (Cp* and Ind), and the carboranyl anion present in complexes **4** are isolobal and uninegative

* Corresponding author. Tel.: +32-4-366-34-195; fax: +32-4-366-3497.
E-mail addresses: A.Demonceau@ulg.ac.be (A. Demonceau), teixidor@icmab.es (F. Teixidor).
[1] O.T. is enrolled in the PhD program of the UAB.
[2] Present address: UCB Chemicals, Research and Technology, Anderlechtstraat 33, B-1620 Drogenbos, Belgium.
[3] Also corresponding author. Fax: +34-93/580-5729.

1387-7003/02/$ - see front matter © 2002 Elsevier Science B.V. All rights reserved.
PII: S1387-7003(02)00608-1

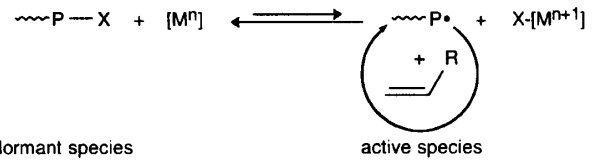

Scheme 1.

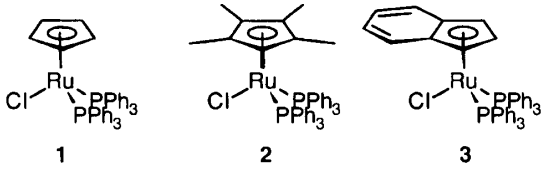

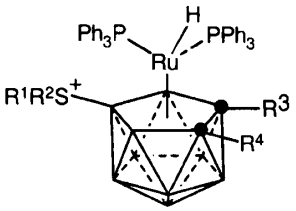

4

	R^1, R^2	R^3	R^4
(a)	CH_3	H	H
(b)	C_2H_5	H	H
(c)	C_2H_5, C_6H_5	H	H
(d)	$(CH_2)_4$	H	H
(e)	CH_3	CH_3	H
(f)	C_2H_5	CH_3	H

Scheme 2.

ligands. Upon $Cp^{\#}$ substitution, it is expected to modify the electronic contributions in these systems. The higher electron donating ability of Cp* compared to Cp is well-established [10], and the capacity of carboranyl ligands ($[C_2B_9H_{11}]^{2-}$) to stabilise uncommon and high oxidation states of the metals as well [11]. (2) On the other hand, $Cp^{\#}$ substitution also results in changing the steric properties of the ligands, which are expressed by the cone angle. In this way, Cp* is obviously bulkier than Cp and, most probably, than the carboranyl ligand $[C_2B_9H_{11}]^{2-}$ [12a,12b], although the relative size of the latter compared to Cp and Cp* is still a question under debate [12c,12d]. The indenyl ligand poses a more complex problem since it is known to undergo a facile metal ring slippage from η^5- to η^3-coordination, leading to the creation of a vacant coordination site on the metal to host an entering ligand or substrate [13a,13b].

Half-sandwich ruthenium complexes **1–4** were employed as catalysts to survey the scope of the radical polymerisation of styrene and *n*-butyl acrylate and to better apprehend the role of the $Cp^{\#}$ ligand. Styrene was polymerised with the $Cp^{\#}$-based complexes in conjunction with (1-bromoethyl)benzene ($PhCHBrCH_3$) as an initiator, whereas ethyl 2-bromopropionate ($CH_3CHBrCO_2C_2H_5$) was employed for initiating the polymerisation of *n*-butyl acrylate. Polymerisation reactions were carried out at 85 or 110 °C (according to the monomer) for 16 h. As illustrated in Table 1, $RuCl(Cp^*)(PPh_3)_2$ (**2**) provided with both monomers an efficiency that greatly surpassed that of related complexes (**1**, **3** and **4**). For instance, **2** led to a rather slow polymerisation of styrene (27% yield), but the polymer thus obtained had a very narrow molecular weight distribution (MWD), $M_w/M_n = 1.1$. In addition, complex **2** also proved to be a markedly active and excellent catalyst precursor which induced the controlled polymerisation of *n*-butyl acrylate in high yield (91%) and with a

Table 1
Ruthenium-catalysed polymerisation of styrene and *n*-butyl acrylate

Complex	Styrene[a]			*n*-Butyl acrylate[a]		
	Polymer yield (%)	M_n[b]	M_w/M_n[b]	Polymer yield (%)	M_n[b]	M_w/M_n[b]
1	10	9,000	1.7	4	1,500	1.35
2	27	11,000	1.10	91	36,000	1.20
3	57	35,000	1.55	67	46,000	2.15
4a	88	21,200	3.05	99	23,100	6.7
4b	25	8,200	1.5	100	56,000	7.1
4c	40	3,900	1.8	97	22,800	1.7
4d	22	9,900	2.1	97	22,500	7.3
4e	25	10,300	2.1	99	78,000	6.1
4f	54	21,000	2.7	100	23,600	5.3

[a] Reaction conditions. $[styrene]_0:[initiator]_0:[Ru]_0 = 750:2:1$ (initiator, (1-bromoethyl)benzene; temperature, 110 °C; reaction time, 16 h). $[n\text{-butyl acrylate}]_0:[initiator]_0:[Ru]_0 = 600:2:1$ (complexes **1–3**) or 1200:4:1 (complexes **4**) (initiator, ethyl 2-bromopropionate; temperature, 85 °C; reaction time, 16 h).

[b] Determined by size-exclusion chromatography (SEC) with polystyrene and PMMA calibration, respectively.

high degree of control ($M_w/M_n = 1.2$). The initiation efficiency was close to unity as indicated by the observation that the number-average molecular weights (M_n) agreed very well with the calculated values, assuming that one molecule of the initiator generates one living polymer chain. Far more important is the establishment that $RuCl(Cp^*)(PPh_3)_2$ (**2**) is by far the most efficient ruthenium-based catalyst for the controlled radical polymerisation of acrylates, and is superior to the reported [$RuCl_2$(*p*-cymene)($PiPr_3$)] [5a,8b] that gives broader MWDs ($M_w/M_n = 1.4$), and previously set the standards in the field.

In contrast, the Cp complex **1** was a much less active catalyst than **2**, while ruthenacarboranes (**4**) were more active. Thus, the activity decreases in the order: **4** > **2** > **1**. In addition, ruthenacarboranes **4** gave polymers with uncontrolled molecular weights and very broad molecular weight distributions. With styrene, polymerisations proceeded smoothly. However, with *n*-butyl acrylate, the polymerisations were much faster. In some cases, the GPC (gel permeation chromatography) curves of the polymers clearly showed some shoulder(s) at higher or lower elution times compared to the main peak, or both (Figs. 1 and 2). In few cases, a bimodal distribution was evidenced (Fig. 2). In light of these observations, we carried out the polymerisation of *n*-butyl acrylate at lower temperatures. Complex **4d** was used as the catalyst, and induced fast polymerisations at a temperature as low as 30 °C (Table 2). However, whatever the temperature, polymerisations were never controlled. Quite interesting was the influence of the temperature on both M_n and M_w/M_n (Fig. 2). At 30 °C, M_n was quite high (~850,000), indicating a low initiation efficiency. As the temperature increased, M_n decreased and M_w/M_n became broader, reaching 6 at 60 °C. Meanwhile, the GPC profiles changed from monomodal at 30 °C to bimodal at 75 °C (Fig. 2). These fast reactions and the broadening of the molecular weight distribution may result from the intrinsic nature of the carboranyl ligands, which are characterised by their high electron-donating ability and their capacity to stabilise transition metals in higher oxidation states. Thus, enhanced stabilisation of the Ru(III) species (Scheme 1) would lead to a higher concentration of radical species, resulting in side reactions such as disproportionation of the growing radical species or β-H elimination from the radical species.

In conclusion, $RuCl(Cp^*)(PPh_3)_2$ (**2**) is a highly efficient catalyst precursor for the controlled radical polymerisation of styrene and *n*-butyl acrylate. On the contrary, related half-sandwich ruthenium complexes (**1**, **3** and **4**) are inefficient and afford polymers in an uncontrolled way. Of particular mechanistic interest are ruthenacarboranes (**4**), which polymerise *n*-butyl acrylate even around room temperature. Complexes **1–4** are now under investigation by cyclic voltammetry analysis with the aim to establish a relationship between catalyst efficiency and $E_{1/2}$ and to find the optimal value of $E_{1/2}$ for observing controlled ATRP mediated by half-sandwich ruthenium complexes.

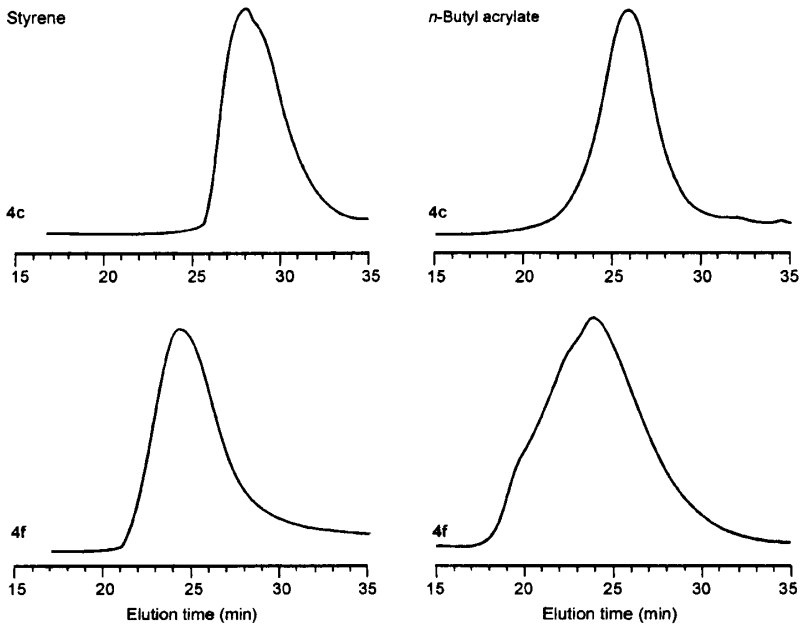

Fig. 1. GPC curves of polystyrenes and poly(*n*-butyl acrylate)s obtained using complexes **4c** and **4f** (reaction conditions same as in Table 1).

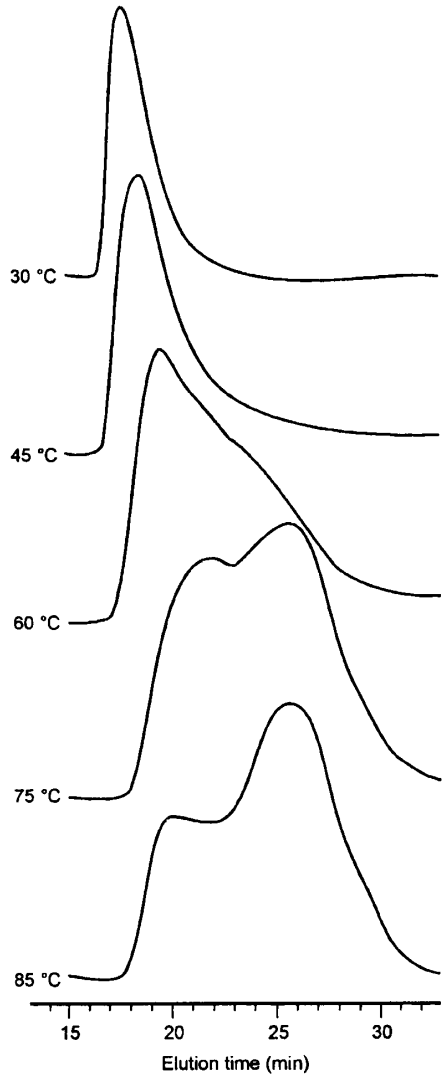

Fig. 2. GPC curves of poly(*n*-butyl acrylate)s obtained using complex **4d** at various temperatures (reaction conditions same as in Table 2).

Table 2
Polymerisation of *n*-butyl acrylate catalysed by complex **4d** and initiated by ethyl 2-bromopropionate[a]

Temperature (°C)	Polymer yield (%)	M_n[b]	M_w/M_n[b]
30	87	835,000	2.65
45	96	250,000	5.15
60	97	71,000	6.1
75	98	23,100	6.7
85	97	22,500	7.3

[a] Same as in Table 1.
[b] Same as in Table 1.

Acknowledgements

This work was financially supported by a grant-in-aid (O.T.) joined to the project MAT98-0921 from CICYT (Spain). Part of this work has also been carried out in the framework of the COST D17/0006/00 and TMR-HPRN CT 2000-10 'Polycat' programmes. The Belgian team is also grateful to the 'Fonds National de la Recherche Scientifique' (F.N.R.S.), Brussels, for the purchase of major instrumentation.

References

[1] M. Kato, M. Kamigaito, M. Sawamoto, T. Higashimura, Macromolecules 28 (1995) 1721–1723.
[2] J.-S. Wang, K. Matyjaszewski, J. Am. Chem. Soc. 117 (1995) 5614–5615.
[3] (a) K. Matyjaszewski, J. Xia, Chem. Rev. 101 (2001) 2921–2990;
(b) M. Kamigaito, T. Ando, M. Sawamoto, Chem. Rev. 101 (2001) 3689–3745.
[4] (a) F. Simal, S. Sebille, A. Demonceau, A.F. Noels, R. Núñez, M. Abad, F. Teixidor, C. Viñas, Tetrahedron Lett. 41 (2000) 5347–5351;
(b) F. Simal, A. Demonceau, A.F. Noels, in: S.G. Pandalai (Ed.), Recent Research Developments in Organic Chemistry, vol. 3, Transworld Research Network, Trivandrum, 1999, pp. 455–464.
[5] (a) F. Simal, A. Demonceau, A.F. Noels, Angew. Chem. 111 (1999) 559–562; Angew. Chem. Int. Ed. 38 (1999) 538–540;
(b) F. Simal, L. Delaude, D. Jan, A. Demonceau, A.F. Noels, Polym. Prepr. Am. Chem. Soc. Div. Polym. Chem. 40 (2) (1999) 336–337;
(c) F. Simal, D. Jan, A. Demonceau, A.F. Noels, in: Controlled/Living Radical Polymerization: Progress in ATRP, NMP, and RAFT, in: K. Matyjaszewski (Ed.), ACS Symposium Series, vol. 768, American Chemical Society, Washington, DC, 2000, pp. 223–233;
(d) F. Simal, S. Sebille, L. Hallet, A. Demonceau, A.F. Noels, Macromol. Symp. 161 (2000) 73–85;
(e) F. Simal, D. Jan, L. Delaude, A. Demonceau, M.-R. Spirlet, A.F. Noels, Can. J. Chem. 79 (2001) 529–535.
[6] (a) F. Simal, A. Demonceau, A.F. Noels, Tetrahedron Lett. 40 (1999) 5689–5693;
(b) F. Simal, S. Delfosse, A. Demonceau, A.F. Noels, K. Denk, F.J. Kohl, T. Weskamp, W.A. Herrmann, Chem. Eur. J. 8 (2002) 3047–3052.
[7] (a) H. Takahashi, T. Ando, M. Kamigaito, M. Sawamoto, Macromolecules 32 (1999) 3820–3823;
(b) Y. Watanabe, T. Ando, M. Kamigaito, M. Sawamoto, Macromolecules 34 (2001) 4370–4374.
[8] (a) F. Simal, L. Wlodarczak, A. Demonceau, A.F. Noels, Tetrahedron Lett. 41 (2000) 6071–6074;
(b) F. Simal, Ph.D Thesis, University of Liège, 2000;
(c) F. Simal, L. Wlodarczak, A. Demonceau, A.F. Noels, Eur. J. Org. Chem. (2001) 2689–2695.
[9] O. Tutusaus, S. Delfosse, A. Demonceau, A.F. Noels, R. Núñez, C. Viñas, F. Teixidor, Tetrahedron Lett. 43 (2002) 983–987.
[10] S.A. Serron, L. Luo, C. Li, M.E. Cucullu, E.D. Stevens, S.P. Nolan, Organometallics 14 (1995) 5290–5297.
[11] A.K. Saxena, N.S. Hosmane, Chem. Rev. 93 (1993) 1081–1124.
[12] (a) M.F. Hawthorne, D.C. Young, T.D. Andrews, D.V. Howe, R.L. Pilling, A.D. Pitts, M. Reintjes, L.F. Warren Jr., P.A. Wegner, J. Am. Chem. Soc. 90 (1968) 879–896;

(b) D. White, N.J. Coville, Adv. Organomet. Chem. 36 (1994) 95–158;
(c) T.P. Hanusa, Polyhedron 1 (1982) 663–665;
(d) D.J. Crowther, N.C. Baenziger, R.F. Jordan, J. Am. Chem. Soc. 113 (1991) 1455–1457.

[13] (a) M.E. Rerek, L.-N. Ji, F. Basolo, J. Chem. Soc. Chem. Commun. (1983) 1208–1209;
(b) M.J. Calhorda, C.C. Romão, L.F. Veiros, Chem. Eur. J. 8 (2002) 868–875.

Annex

Annex

(Treballs publicats posteriorment
a la comissió de Doctorat d'abril de 2003)

The Modulating Possibilities of Dicarbollide Clusters. Optimizing the Kharasch Catalysts

Oscar Tutusaus,[†,‡] Clara Viñas,[†] Rosario Núñez,[†] Francesc Teixidor,*[†] Albert Demonceau,[§] Sébastién Delfosse,[§] Alfred F. Noels,[§] Ignasi Mata,[†] Elies Molins[†]

Institut de Ciència de Materials de Barcelona (CSIC), Campus de la U.A.B, 08193 Bellaterra, Spain; Laboratory of Macromolecular Chemistry and Organic Catalysis, University of Liège, Sart-Tilman (B.6a), B-4000 Liège, Belgium.

E-mail: teixidor@icmab.es

The structurally and coordinatively similar dicarbollide $[7,8\text{-}C_2B_9H_{11}]^{2-}$ (Dcb)[1] and cyclopentadienyl ligands $[C_5R_5]^-$ ($Cp^{\#}$)[1] differ in their capacity to stabilize high oxidation states and the out of plane disposition of the open face substituents.[1,2] These differences offer new alternatives in fields where Cp is a basic participant, and in which association/dissociation of ligands,[3] and electron capture/release are key steps. In the Kharasch reaction, also known as Atom Transfer Radical Addition (ATRA),[4] the above mentioned steps are fundamental. This is why ATRA reaction was chosen to compare Dcb and Cp options. To date some of the more active ATRA catalysts contain Cp like ligands, e.g. $[RuClCp^{\#}(PR_3)_2]$ ($Cp^{\#}$ = Cp (**1**), Cp* (**2**) and indenyl (**3**)).[4b,5] Substitution of one open face hydrogen by a SR_2 in Dcb equals the charge of Cp and leads to the new monoanionic dicarbollide, $[R_2S\text{-}7,8\text{-}C_2B_9H_{10}]^-$. We have chosen the most symmetrical position to locate the R_2S group, although other positions are also possible,[6] and $[10\text{-}R^1R^2S\text{-}7\text{-}R\text{-}7,8\text{-}C_2B_9H_9]^-$ (**4a-f**) derivatives were synthesized.[7] Reaction of these ligands with $[RuCl_2(PPh_3)_3]$ in ethanol led to complexes with the $[3\text{-}H\text{-}3,3\text{-}(PPh_3)_2\text{-}8\text{-}SR^1R^2\text{-}1\text{-}R\text{-}3,1,2\text{-}RuC_2B_9H_9]$ (**5a-f**) general stoichiometry (Scheme 1). All complexes **5a-f**, were characterized by NMR techniques and the structure of **5a** (Figure 1) was determined by X-ray structure analysis. Crystals of **5a** were grown from a solution of CH_2Cl_2/hexane.

Scheme 1. Preparation of complexes **5a-f**.

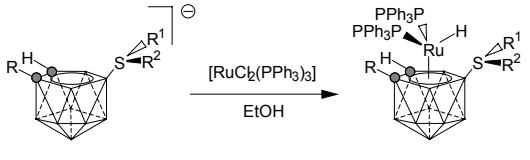

4a-f **5a-f**

a: R=H, R^1=R^2=Me
b: R=H, R^1=R^2=Et
c: R=H, R^1=Et, R^2=Ph
d: R=H, R^1=R^2=$(CH_2)_2$
e: R=Me, R^1=R^2=Me
f : R=Me, R^1=R^2=Et

The ^{11}B NMR of complexes with R=H and R^1=R^2 (**5a**, **5b**, **5d**) displays a 1:1:1:3:3 pattern in agreement with a C_s symmetry. The crystal structure determination of **5a** $[3\text{-}H\text{-}3,3\text{-}(PPh_3)_2\text{-}8\text{-}SMe_2\text{-}3,1,2\text{-}RuC_2B_9H_{10})]$ unambiguously indicated that the metal hydride pointed towards sulfur (Figure 1). Distances and angles of **5a** are very similar to the non-compensated anion $[3\text{-}H\text{-}3,3\text{-}(PPh_3)_2\text{-}3,1,2\text{-}RuC_2B_9H_{11}]^-$ (**6**$^-$),[8] Ru-P (2.321(3) and 2.298(3) Å vs. 2.322 and 2.294 Å) and Ru-H (1.600(90) vs. 1.679 Å). The Ru distance to the C_2B_3 open face is 1.735(5) Å for **5a** and 1.771 Å for **6**. The Ru-B and Ru-C distances in **5a** are very similar, from 2.203(11) to 2.307(10) Å. Therefore the pendant R_2S^+- group has not produced significant geometric changes in the complex. In support of this is the similar angle between the B(8)-S and the C_2B_3 plane for **5a** (14.2º) and **4a** (17.1º).[7] This implies that in the event one PPh_3 was dissociated, the long 3.435(3) Å S-Ru distance in **5a**, larger than the van der Waals radii, should prevent a S-Ru contact.

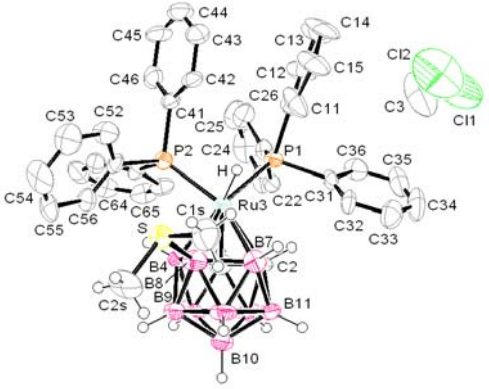

Figure 1. Molecular structure of **5a**·CH_2Cl_2 showing the atom labeling scheme.

The Kharasch addition of CCl_4 to methyl methacrylate (MMA) and styrene (Sty) double bonds has been done to compare the catalytic activity of **5a-f** with **2**, considered to be the fastest and highest Kharasch conversion capacity Ru complex.[4b] All **5a-f** complexes are superior in all aspects to **2**, as shown in Table 1.

In particular for **5c** and with regard to MMA and Sty, total turnover numbers (TTN) of 4200 and 9000, and initial turnover frequencies (TOF) of 1880 and 1500 h^{-1} were obtained at 40 ºC, respectively, as opposed to maximum TTN of 1600-1700 and TOF of 400 h^{-1} observed for **2**.[4b] In addition, the TTN for **5c** is even higher than the one obtained for the pincer N,C,N-chelating aryldiaminonickel complex, to this moment the most efficient ATRA catalyst reported, with TTN of 1730 and TOF of 400 h^{-1} for MMA.[9] Once proven the superior possibilities of **5c** for this type of reaction it remained to be disclosed whether it is due to: i) the capacity of R_2S^+- to donate two electrons to the metal after dissociation of one phosphine; ii) the fine tuning to optimal potential in the Ru catalyst made by $[10\text{-}R_2S\text{-}7,8\text{-}C_2B_9H_{10}]^-$ or iii) to a combination of both.

† Institut de Ciència de Materials de Barcelona, CSIC.
‡ O. Tutusaus is enrolled in the UAB PhD Program.
§ University of Liège.

Table 1. Cyclic voltammetry[a] data and Kharasch addition of carbon tetrachloride to styrene and methyl methacrylate [b]

ΔE [mV]	E° [mV]	Catalyst	Conversion[c] [%] / Yield[c] [%]	
			Styrene	MMA
86	+133	**1**	24/10	62/5
94	-83	**2**	86/69	79/79
94	-10	**3**	74/69	83/83
76	-266	**5a**	100/99	98/94
82	-266	**5b**	100/99	98/94
98	-287	**5c**	100/99	100/100
80	-266	**5d**	100/99	99/99
80	-366	**5e**	100/99	92/84
88	-368	**5f**	100/99	92/84

[a] Sample, 1 mM; Bu_4NPF_6 (0.1M) in CH_2Cl_2 ; ν =50 mVs^{-1}; potentials are reported in millivolt versus ferrocene as an internal standard. [b] Reaction conditions: olefin (9 mmol), carbon tetrachloride (13 mmol), catalyst (0.03 mmol), toluene (4 mL), dodecane (0.25 mL), under nitrogen atmosphere. The reactions were carried out at 40°C and stopped after 6 h.[c] Conversions and yields are based on the olefin, and determined by GC using dodecane as internal standard. The Kharasch adducts were characterized by comparison with literature data.[4b]

Point i) was addressed by adding free PPh_3 to the reaction mixture, reasoning that addition of phosphine would decrease the rate dramatically, as observed in reactions in which a phosphine dissociative pathway is operative.[4a,10,11] Addition of up to 12 equiv. of PPh_3 per equiv. of catalyst in reactions catalyzed by **5a** and **5c** slowed the reaction rate (Figure 2a) in a manner parallel to **2** (Figure 2b). Complex **2** does not have the capacity to internally satisfy the electronic demands of a complex having lost one ancillary ligand. Being the behavior of **5a**/**5c** parallel to **2** we considered that the stabilizing capacity of the R_2S^+- group upon ligand's dissociation could be discarded, in agreement with the structural data discussed earlier.

Possibility ii) was addressed correlating the E° values for the $Ru^{II} \rightarrow Ru^{III}$ process with the catalytic Kharasch activity towards a common substrate. Cyclic voltammetry data are displayed in Table 1. Based on this data, the activity catalyst order is **5a-d** > **5e-f** > **2**,**3** > **1**. Interestingly, groupings of catalysts can be made, both from the catalytic activity side, and from the E° point of view. In this way, **5a-d** have E°'s near –270 mV, and are the most active catalysts; close in activity are **5e** and **5f** with E°'s near -370 mV. Consequently catalyst precursors with E°'s near –370 mV are not as efficient as these with E°'s near –270 mV, but all of them are more efficient than **2**, **3** and **1** with E°'s between –83 mV and +133 mV. The fact that the highest catalytic activity is found not in one edge of E°'s values nor in the other, but in between, implies that both species, Ru^{II} and Ru^{III}, must be equally stabilized by the same ligand system, and that for a maximum of efficiency of the catalytic conversion process E° must be in a narrow range of potentials. In this way **2** and **3** are more efficient than **1** confirming that the closer to –270 mV is E°, the best for a maximum catalytic performance. This proves that a direct relationship between ATRA catalyst efficiency and E° does exist for these complexes.

Charge-compensated carborane ligands have thus allowed to adequately tune the E° values of the $Cp^\#$ ligands, permitting to reach through *exo*-cluster substitution the necessary potential; but it is our interpretation that this has been possible through a to-and-fro electron density movement, facilitated by the uniqueness of the boron cluster-sulfonium bridge. We believe that the capacity to donate and to retrieve electron density from the metal makes the [10-R_2S-7,8-$C_2B_9H_{10}$]$^-$ system very adequate when two oxidation states require to be stabilized by the same ligand system in different steps of a catalytic process.

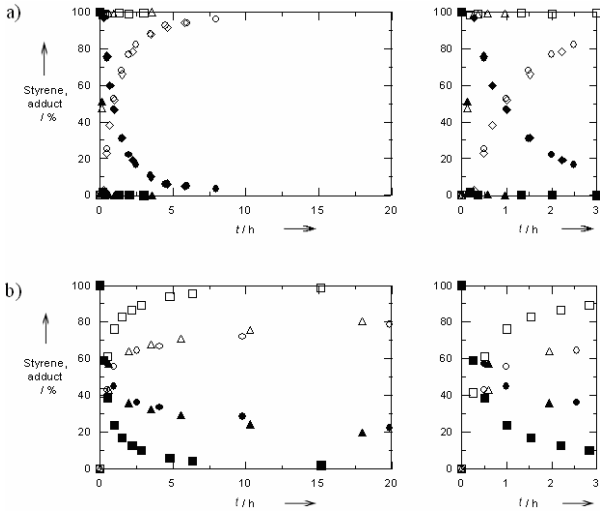

Figure 2. Styrene (■,●,▲,◆) and adduct (□,○,△,◇) vs. time for the Kharasch addition of CCl_4 to styrene at 40 ºC catalysed by complexes **5a**, **5c** and **2** without PPh_3 and in the presence of 12 equiv. PPh_3. a) Complex **5a** without PPh_3 (■,□) and with 11.9 equiv. PPh_3 (●,○); complex **5c** without PPh_3 (▲,△) and with 12.1 equiv. PPh_3 (◆,◇). b) **2** without PPh_3 (■,□), with 12.05 (▲,△) and 12.4 equiv. PPh_3 (●,○).

Acknowledgment. This work has been supported by CICYT, MAT01-1575 and Generalitat de Catalunya, 2001/SGR/00337

Supporting Information Available. Crystallographic data of **5a** is available free of charge via the Internet http://pubs.acs.org.

(1) Hawthorne, M. F.; Young, D. C.; Andrews, T. D.; Howe, D. V.; Pilling, R. L.; Pitts, A. D.; Reintjes, M.; Warren,L. F.; Wegner, Jr. P.A. *J. Am. Chem. Soc.* **1968**, *90*, 879.
(2) (a) Teixidor, F.; Viñas, C.; Abad, M. M.; Kivekäs, R.; Sillanpää, R. *J. Organomet. Chem.* **1996**, *509*, 139. (b) Viñas, C.; Nuñez, R.; Teixidor, F.; Sillanpää, R.; Kivekas, R. *Organometallics* **1999**, *18*, 4712.
(3) The association/dissociation step is required for 18 e$^-$ complexes. It is perhaps not so necessary for 16 e$^-$ complexes.
(4) (a) Bland, W. J; Davis, R.; Durrant, J. L. A. *J. Organomet. Chem.* **1985**, *280*, 397. (b) Simal, F.; Wlodarczak, L.; Demonceau, A.; Noels, A. F. *Eur. J. Org. Chem.* **2001**, 2689.
(5) Simal, F.; Wlodarczak, L.; Demonceau, A.; Noels, A. F. *Tetrahedron Lett.* **2000**, *41*, 6071.
(6) (a) Cowie, J.; Hamilton, E. J. M.; Laurie, J. C. V.; Welch, A. J. *J. Organomet. Chem.* **1990**, *394*, 1. (b) Douek, N. L.; Welch, A. J. *J. Chem. Soc. Dalton Trans.* **1993**, 1917. (c) Yan, Y. -K.; Mingos, D. M. P.; Müller, T. E.; Williams, D. J.; Kurmoo, M. *J. Chem. Soc. Dalton Trans.* **1994**, 1735. (d) Dunn, S.; Garrioch, R. M.; Rosair, G. M.; Smith, L.; Welch, A. J. *Collect. Czech. Chem. Commun.* **1999**, *64*, 1013.
(7) Tutusaus, O.; Teixidor, F.; Núñez, R.; Viñas, C.; Sillanpää, R.; Kivekäs, R. *J. Organomet. Chem.* **2002**, *657*, 247.
(8) Chizhevsky, I. T.; Lobanova, I. A.; Petrovskii, P. V.; Bregadze, V. I.; Dolgushin, F. M.; Yanovsky, A.; Struchkov, I. Y. T.; Chistyakov, A. L.; Stankevich, I. V. *Organometallics* **1999**, *18*, 726.
(9) (a) van de Kuil, L. A.; Grove, D. M.; Gossage, R. A.; Zwikker, J. W.; Jenneskens, L. W.; Drenth, W.; van Koten, G. *Organometallics* **1997**, *16*, 4985. (b) Gossage, R. A.; van de Kuil, L. A.; van Koten, G. *Acc. Chem. Res.* **1998**, *31*, 423.
(10) Teixidor, F.; Flores, M. A.; Viñas, C.; Sillanpää, R.; Kivekäs, R. *J. Am. Chem. Soc.* **2000**, *122*, 1963.
(11) (a) James, B. R.; Markham, L. D. *Inorg. Chem.* **1974**, *13*, 97. (b) Hoffman, P. R.; Caulton, K. G. *J. Am. Chem. Soc.* **1975**, *97*, 4221. (c) Bland, W. J.; Davis, R.; Durrant, J. L. A. *J. Organomet. Chem.* **1984**, *267*, C45. (d) Dias, E. L.; Nguyen, S. T.; Grubbs, R. H. *J. Am. Chem. Soc.* **1997**, *119*, 3887. (e) Huang, J.; Stevens, E. D.; Nolan, S. P; Petersen, J. L. *J. Am. Chem. Soc.* **1999**, *121*, 2674.

Annex

(Treballs publicats en fonts no pertanyents al SCI)

Controlled radical polymerization catalyzed by ruthenium complexes. Variations on Ru-Cp$^{\#}$

Sébastien Delfosse[1], Aurore Richel[1], François Simal[1,†] Albert Demonceau[1,*], Alfred F. Noels[1], Oscar Tutusaus[2,‡] Rosario Núñez[2], Clara Viñas[2], and Francesc Teixidor[2]

[1] **Laboratory of Macromolecular Chemistry and Organic Catalysis University of Liège, Sart-Tilman (B.6a), B-4000 Liège, Belgium**

[2] **Institut de Ciència de Materials CSIC-UAB, Campus de Bellaterra, Cerdanyola, 08193 Barcelona, Spain**

A series of isoelectronic ruthenium-based complexes of the general formula [RuX(Cp$^{\#}$)L$_2$] (Cp$^{\#}$ = cyclopentadienyl or cyclopentadienyl derivatives) were synthesized, and their relative catalytic activities were determined by monitoring the atom transfer radical polymerization of methyl methacrylate, *n*-butyl acrylate, and styrene. [RuCl(Cp*)(PPh$_3$)$_2$] and [RuCl(Ind)(PPh$_3$)$_2$] were found to be highly efficient catalysts for ATRP, producing polymers with narrow molecular weight distributions (M_w/M_n < 1.2). The following order of increasing efficiency was determined: [RuCl(Cp)(PPh$_3$)$_2$] << [RuCl(Ind)(PPh$_3$)$_2$] < [RuCl(Cp*)(PPh$_3$)$_2$]. In sharp contrast, ruthenacarboranes were inefficient in ATRP, demonstrating therefore the prominent role of the Cp$^{\#}$ ligand. The effect of the phosphine ligands was also investigated, and additional studies indicated that the release of a phosphine ligand occurred prior to the activation of the carbon-halogen bond of both the initiator and polymer growing chain end by the unsaturated ruthenium center.

It was in 1995 that Sawamoto (*1*) and Matyjaszewski (*2*) independently reported their seminal papers on atom transfer radical polymerization (ATRP). Among the numerous catalytic systems developed for ATRP, ruthenium plays a prominent role (*3*). [RuCl$_2$(PPh$_3$)$_3$] (**A**, Scheme 1) was the first complex employed for the metal-catalyzed controlled radical polymerization of methyl methacrylate in conjunction

* Corresponding author. Fax : ++32-(0)4 366 3497; e-mail : A.Demonceau@ulg.ac.be.
† Present address : UCB Chemicals, Research and Technology, Anderlechtstraat 33, B-1620 Drogenbos, Belgium.
‡ O.T. is enrolled in the PhD program of the UAB.

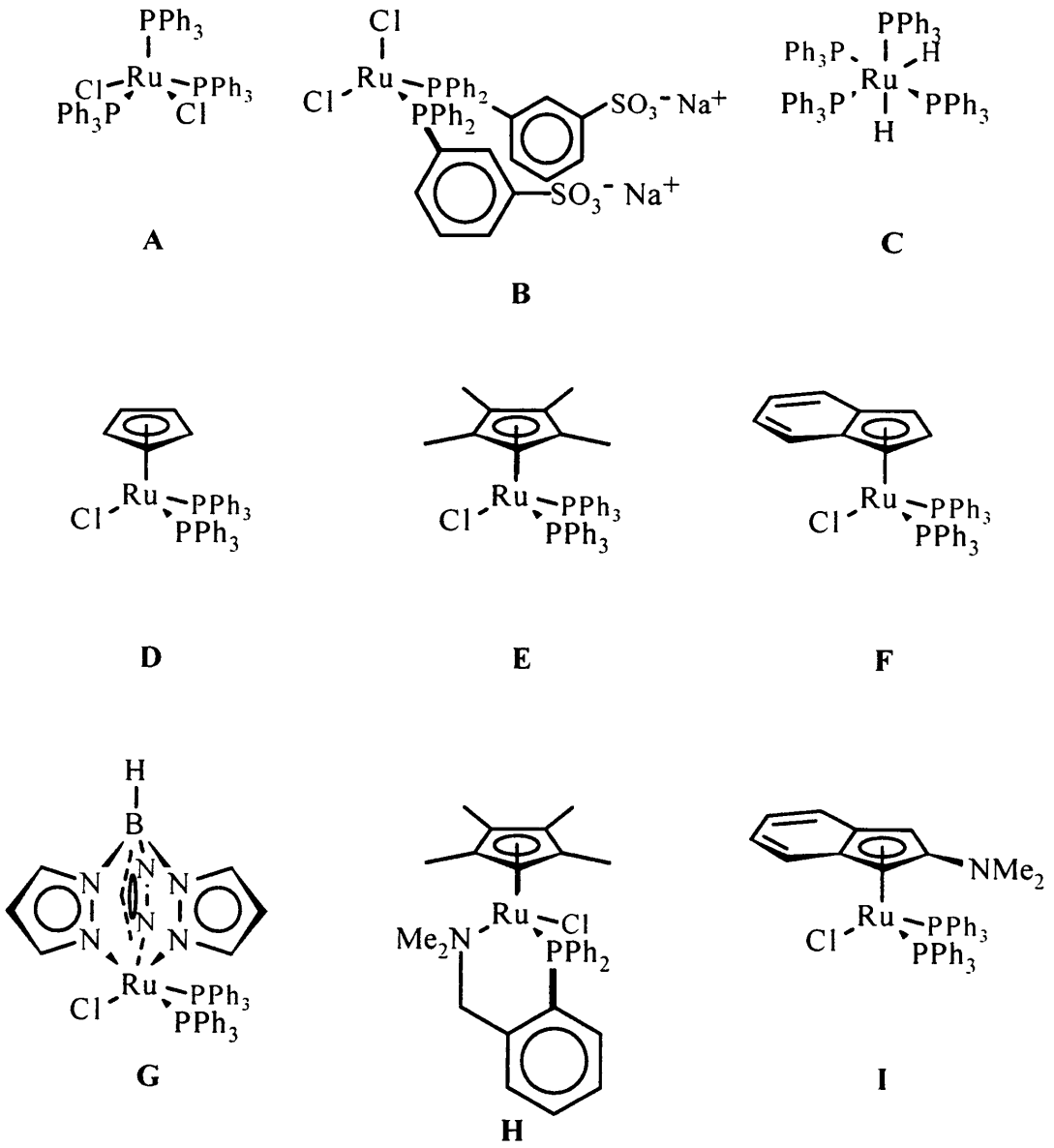

Scheme 1. Representative Sawamoto's ruthenium complexes for ATRP

with CCl_4 as an initiator in the presence of a Lewis acid as an additive. Since then, the development of new ruthenium catalysts for ATRP has been a dramatic success (Scheme 1). Interestingly, half-sandwich ruthenium complexes (**D-F**) proved very successful, with the indenyl derivative (**F**) providing the fastest controlled radical polymerization of methyl methacrylate *without* Lewis acid activation. Furthermore, addition of an amine such as *n*-Bu_2NH dramatically increased the rate so that completion of the polymerization was attained in 5 h at 100 °C without broadening of the molecular weight distributions (*4*). Very recently, Sawamoto disclosed preliminary results obtained using half-metallocene ruthenium complexes with either *P,N*-chelating (**H**) or aminoindenyl ligands (**I**) (*5*).

Back in 1999, we found that the 18-electron complex [$RuCl_2$(*p*-cymene)(PCy_3)] (*p*-cymene = 4-isopropyltoluene) (**1**) was a versatile and efficient catalyst precursor for promoting ATRP of vinyl monomers *without* cocatalyst activation (*6*). We then

moved to $[RuCl_2(=CHPh)(PCy_3)_2]$, **2**, the Grubbs' ruthenium benzylidene complex which has had a tremendous impact on olefin metathesis. Since initial results showed that complex **2** proved to be highly efficient also for ATRP, we expanded our investigations towards *N*-heterocyclic carbene-containing ruthenium benzylidene complexes, **3** and **4** (*7*). Later on, we also discovered (independently of Sawamoto)

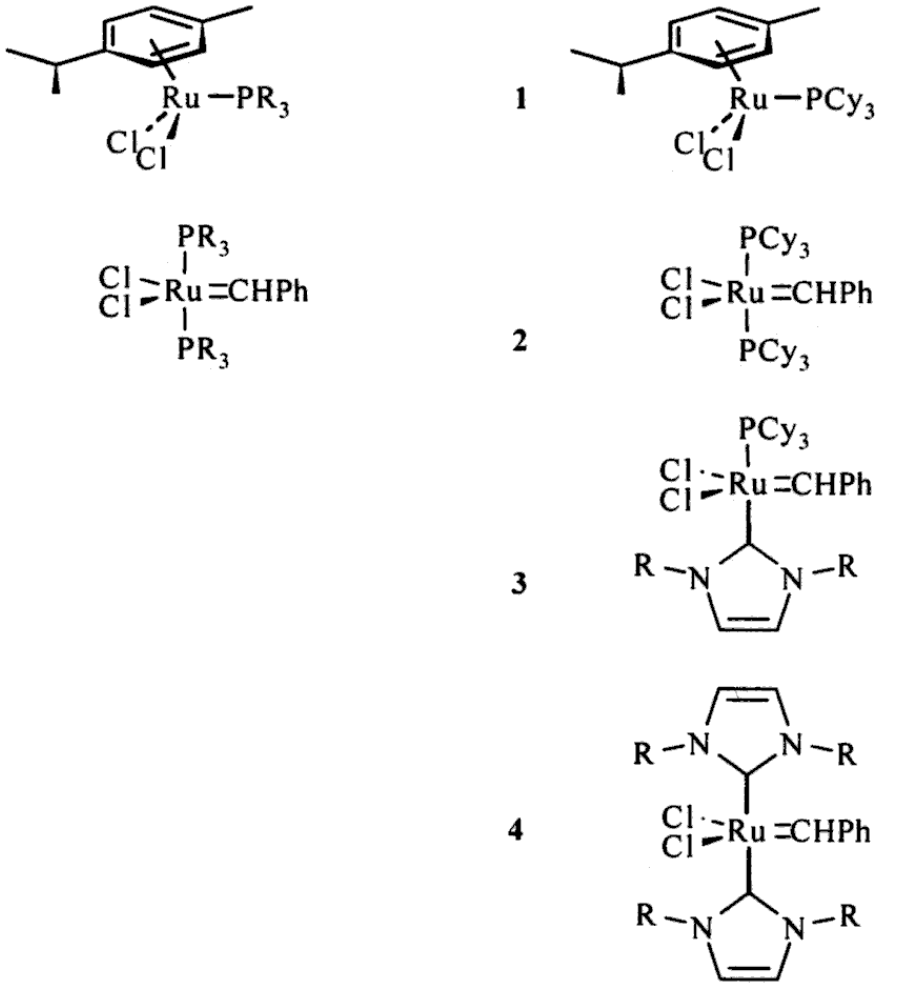

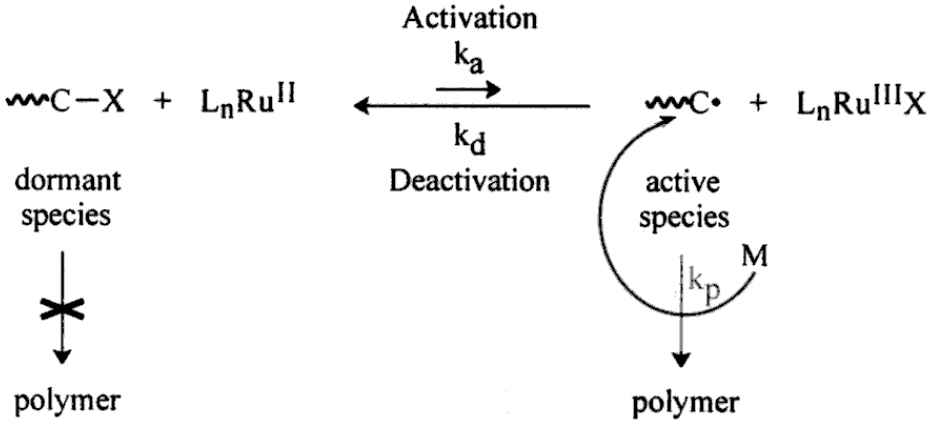

Scheme 2. Generally accepted mechanism for ATRP

that half-sandwich ruthenium complexes, [RuCl(Cp$^{\#}$)(PPh$_3$)$_2$], were efficient and markedly active catalysts for ATRP (*8*).

Since ATRP is based on a dynamic equilibration between active propagating radicals and dormant species (Scheme 2), it is anticipated that catalytic engineering at the metal center should shift this equilibrium to the most suitable position, so as to maintain a low concentration of propagating radicals while keeping a useful rate of polymerization for polymers to be obtained on a sensible time-scale. To further improve the catalyst efficiency in the ATRP process, we have launched a detailed investigation on the role of the ligands in complexes of the general formula [RuX(Cp$^{\#}$)LL'] (Scheme 3). The present contribution is aiming at illustrating how variation of the cyclopentadienyl-based ligand (Cp$^{\#}$), ancillary ligands LL' (phosphine or carbon monoxide), and X (chloride, hydride, or allyl) influences ATRP of vinyl monomers, such as methyl methacrylate, *n*-butyl acrylate, and styrene.

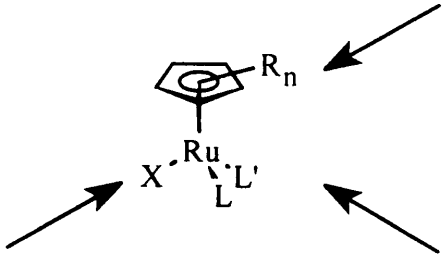

Scheme 3. Tuning of ruthenium-cyclopentadienyl derivatives

Chemical Engineering of [RuX(Cp$^{\#}$)LL'] Complexes

Influence of the Cp$^{\#}$ ligand

Nowadays, the factors governing catalyst activity and the mechanism by which half-sandwich ruthenium catalysts perform radical reactions are not known. Investigations were undertaken to address both of these topics in the following way: By varying the ligand sphere around the ruthenium catalyst, we wished to determine how the electronic and steric properties of the ligands affect catalyst activity.

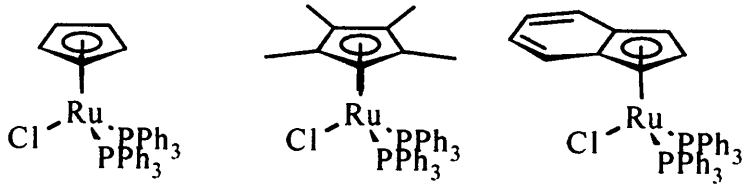

5 **6** **7**

Ruthenium complexes **5**–**7** and ruthenacarboranes **8** were compared for two reasons: (1) The cyclopentadienyl anion (Cp), its pentamethylcyclopentadienyl (Cp*) and indenyl (Ind) derivatives, and the carboranyl anion present in complexes **8** are isolobal and uninegative ligands. Upon Cp$^{\#}$ substitution, it is expected to modify the electronic contributions in these systems. The higher electron donating ability of Cp* compared to Cp is well-established, and the capacity of carboranyl ligands

($[C_2B_9H_{11}]^{2-}$) to stabilize uncommon and high oxidation states of the metals as well. (2) On the other hand, $Cp^{\#}$ substitution also results in changing the steric properties of the ligands, which are expressed by the cone angle, θ (Scheme 4). In this way, Cp* is obviously bulkier than Cp and, most probably, than the carboranyl ligand $[C_2B_9H_{11}]^{2-}$, although the relative size of the latter compared to Cp and Cp* is still a question under debate.

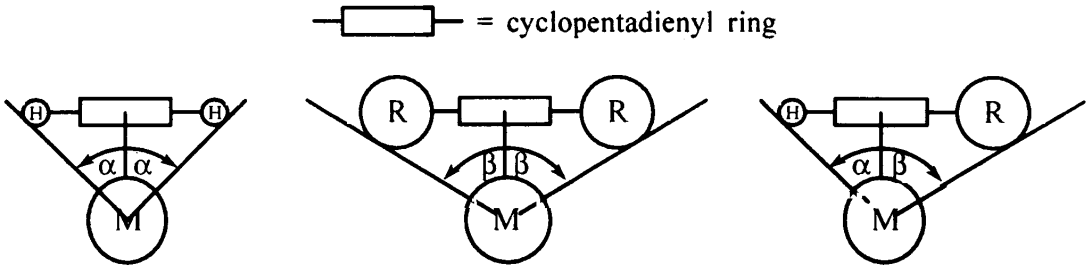

Scheme 4. Cone angle (θ) for the cyclopentadienyl ring, C_5H_5, a pentasubstituted cyclopentadienyl ring, C_5R_5, and measurement of the average cone angle for an n substituted cyclopentadienyl ring, $C_5H_{5-n}R_n$ (*9*)

The indenyl ligand poses a more complex problem since it is known to undergo a facile metal ring slippage from η^5- to η^3-coordination, leading to the creation of a vacant coordination site on the metal to host an entering ligand or substrate (Scheme 5) (*10*).

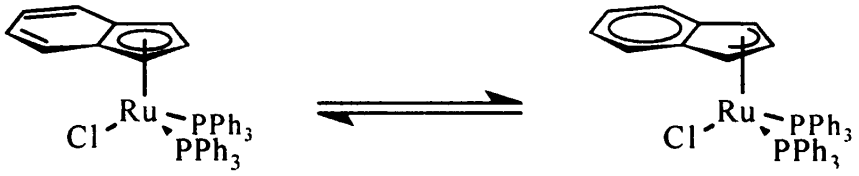

η^5-, 18-electron complex

η^3-, 16-electron complex

Scheme 5. The indenyl effect

First, half-sandwich ruthenium complexes **5**-**7** were employed as catalysts to survey the scope of the radical polymerization of vinyl monomers and to better apprehend the role of the $Cp^{\#}$ ligand. Methyl methacrylate (MMA), *n*-butyl acrylate (BA), and styrene (S) were selected as model vinyl monomers. Ethyl 2-bromo-2-methylpropionate, ethyl 2-bromopropionate, and (1-bromoethyl)benzene were used as initiators for the polymerization of MMA, BA, and S, respectively, because of a structure quite comparable to that of the dormant species of PMMA, PBA, and PS chains. Polymerization reactions were carried out *without* cocatalyst at 85 or 110 °C (according to the monomer) for 16 h.

As illustrated in Table 1, $[RuCl(Cp^*)(PPh_3)_2]$ (**6**) provided an efficiency that generally surpassed that of related complexes, **5** and **7**. For instance, **6** led to a rather slow polymerization of styrene (27 % yield), but the polymer thus obtained had a very narrow molecular weight distribution (MWD, M_w/M_n = 1.10).

Table 1. ATRP of Methyl Methacrylate, *n*-Butyl Acrylate, and Styrene Catalyzed by Half-Sandwich Ruthenium Complexes 5-7

Complex	*Polymer yield (%)*	M_n[d]	M_w/M_n[d]	f[e]
Methyl methacrylate[a]				
5	28	12 000	1.27	0.95
6	19	9 600	1.45	0.80
7	45	21 000	1.30	0.85
n-Butyl acrylate[b]				
5	4	1 500	1.35	0.99
6	91	36 000	1.20	0.95
7	67	46 000	2.15	0.55
Styrene[c]				
5	10	9 000	1.7	0.45
6	27	11 000	1.10	0.95
7	57	35 000	1.55	0.65

[a] $[MMA]_0:[initiator]_0:[Ru]_0$ = 800:2:1 (initiator, ethyl 2-bromo-2-methyl-propionate; temperature, 85 °C; reaction time, 16 h. [b] $[n\text{-Butyl acrylate}]_0:[initiator]_0:[Ru]_0$ = 600:2:1 (initiator, ethyl 2-bromopropionate; temperature, 85 °C; reaction time, 16 h. [c] $[Styrene]_0:[initiator]_0:[Ru]_0$ = 750:2:1 (initiator, (1-bromoethyl)benzene; temperature, 110 °C; reaction time, 16 h. [d] Determined by size-exclusion chromatography (SEC) with PMMA and polystyrene calibration, respectively. [e] f (initiation efficiency) = $M_{n,th}/M_{n,exp}$ with $M_{n,th}$ = ([monomer]$_0$/[initiator]$_0$) x $MW_{momomer}$ x conversion.

Complex **6** also induced the controlled polymerization of *n*-butyl acrylate in high yield (91 %) and with a high degree of control (M_w/M_n = 1.20) (*11*). In addition, in both cases, the initiation efficiency (*f*) was close to unity as indicated by the observation that the number-average molecular weights (M_n) agreed very well with the calculated values, assuming that one molecule of the initiator generates one living polymer chain. With methyl methacrylate, the molecular weight distribution of the obtained polymer was broader (M_w/M_n = 1.45); the GPC curve was bimodal, and also showed additional shoulders.

[RuCl(Cp)(PPh_3)$_2$] (**5**) and [RuCl(Ind)(PPh_3)$_2$] (**7**) were more active than their Cp* analogue (**6**) for MMA polymerization, and gave narrower MWDs. The reverse was observed for the polymerization of *n*-butyl acrylate and styrene, as exemplified by the broadening of the MWDs for PBA (M_w/M_n = 2.15) and PS (M_w/M_n = 1.55) obtained using [RuCl(Ind)(PPh_3)$_2$] as the catalyst.

For several polymerization reactions, the semi logarithmic plots of monomer conversion against time were linear. The linear plots suggest a first-order kinetic with respect to the monomer concentration and that constant radical concentrations were maintained during the reactions. In other cases, a significant deviation from linearity was observed. As shown in Figure 1, in the early stage of MMA polymerization catalyzed by [RuCl(Ind)(PPh_3)$_2$] the $\ln([M]_o/[M])$ vs time plot is linear (y = 0.016087 + 0.077936 x; r^2 = 0.981, for the first five hours of reaction), indicating that the radical concentration remained constant. However, the plot begins to deviate from the

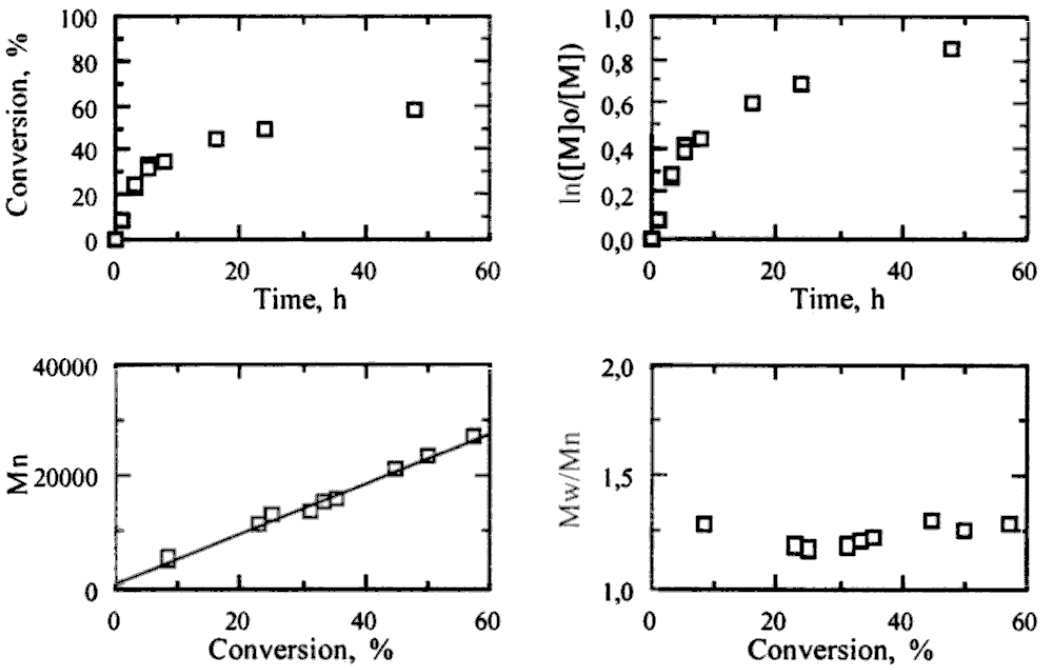

Figure 1. *Polymerization of methyl methacrylate initiated by ethyl 2-bromo-2-methylpropionate and catalyzed by [RuCl(Ind)(PPh$_3$)$_2$] (7), at 85 °C (Reaction conditions same as in Table 1).*

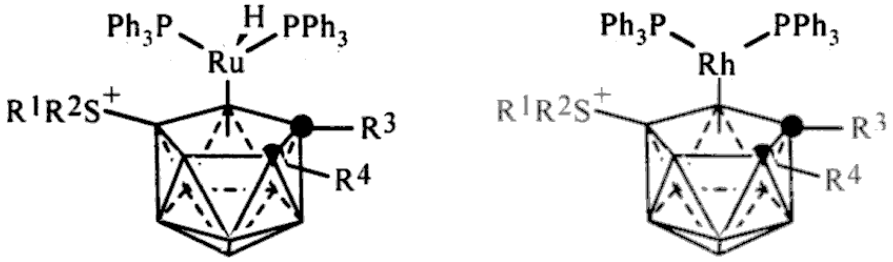

8 **9**

	R^1, R^2	R^3	R^4
(a)	CH_3	H	H
(b)	C_2H_5	H	H
(c)	C_2H_5, C_6H_5	H	H
(d)	$(CH_2)_4$	H	H
(e)	CH_3	CH_3	H
(f)	C_2H_5	CH_3	H

first-order kinetic and slows down at approximately 30 % conversion. This suggests that there is a higher contribution of termination reactions, which results from an

Table 2. ATRP of Methyl Methacrylate, *n*-Butyl Acrylate, and Styrene Catalyzed by Ruthena- (8) and Rhodacarborane (9) Complexes

Complex	Polymer yield (%)	M_n[d]	M_w/M_n	Complex	Polymer yield (%)	M_n[d]	M_w/M_n
Methyl methacrylate[a]							
8a	93	25 700	1.65	**9a**	93	18 300	1.95
8b	93	25 200	1.6	**9b**	93	14 000	1.85
8c	88	18 100	1.65	**9c**	99	25 700	1.9
8d	88	23 400	1.7	**9d**	84	14 800	1.9
8e	94	25 300	1.75	**9e**	86	20 300	1.85
8f	90	28 400	1.65	**9f**	90	20 800	1.85
n-Butyl acrylate[b]							
8a	99	23 100	6.7	**9a**	99	23 600	4.0
8b	99	56 000	7.1	**9b**	97	34 000	1.9
8c	97	22 800	1.7	**9c**	97	36 500	3.0
8d	97	22 500	7.3	**9d**	99	21 800	3.9
8e	99	78 000	6.1	**9e**	95	56 000	5.6
8f	99	23 600	5.3	**9f**	98	40 000	5.1
Styrene[c]							
8a	88	21 200	3.05	**9a**	65	6 700	2.8
8b	25	8 200	1.5	**9b**	51	11 500	2.15
8c	40	3 900	1.8	**9c**	69	18 200	1.85
8d	22	9 900	2.1	**9d**	45	14 800	2.05
8e	25	10 300	2.1	**9e**	77	16 000	1.9
8f	54	21 000	2.7	**9f**	83	25 600	1.6

[a,b,c,d] Reaction conditions same as in Table 1, except for *n*-butyl acrylate : [*n*-butyl acrylate]$_0$:[initiator]$_0$:[complex]$_0$ = 1200:4:1, instead of 600:2:1 (Table 1).

increase in [Ru(III)] and radical concentration.

The molecular weight and polydispersity of PMMA as the functions of monomer conversion are shown in Figure 1. The molecular weight increases linearly with conversion ($y = 418.54 + 454.18\ x$; $r^2 = 0.992$), while MWDs are around 1.2-1.3, reaching a minimum of 1.17 at approximately 25 % conversion.

To further enlarge the set of Cp$^{\#}$ ligands and to better apprehend their impact on the catalytic process, ruthenacarboranes (**8**) were prepared and tested in ATRP (Table 2). With MMA and BA, complexes **8** were more active than complexes **5-7**. With styrene, however, they displayed similar activities, and polymerizations proceeded smoothly. In addition, ruthenacarboranes generally gave polymers with uncontrolled molecular weights and broad (or very broad) molecular weight distributions. In some cases, the GPC curves of the polymers clearly showed some shoulder(s) at higher or lower elution times compared to the main peak, or both (Figure 2). In few cases, especially with PBA, a bimodal distribution was evidenced.

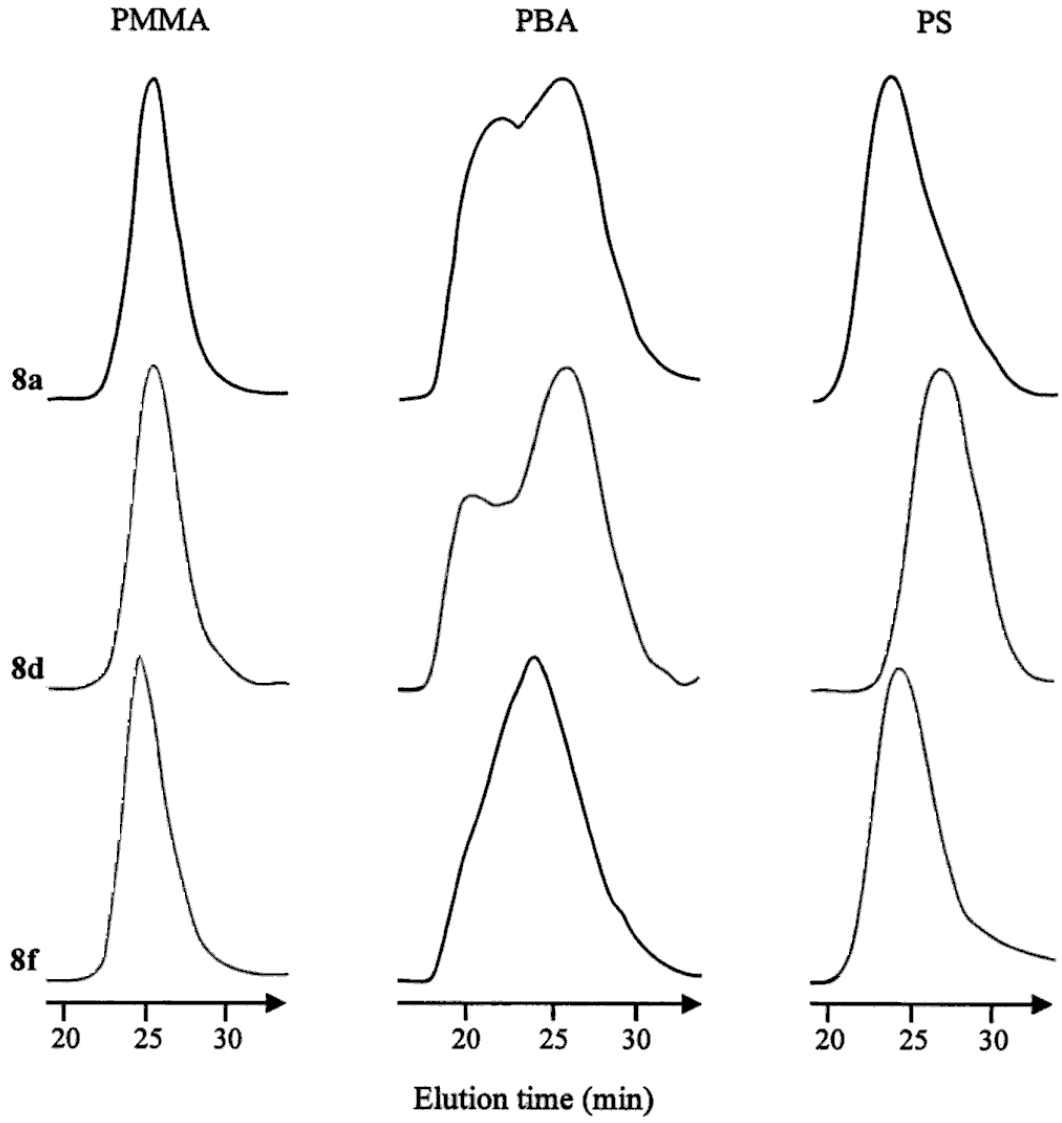

Figure 2. *GPC curves of poly(methyl methacrylate)s, poly(n-butyl acrylate)s, and polystyrenes obtained using complexes* ***8a***, ***8d***, *and* ***8f*** *(Reaction conditions same as in Table 2).*

Table 3. ATRP of *n*-Butyl Acrylate Catalyzed by Rhodacarborane 9d[a]

Temperature (°C)	*Polymer yield (%)*	M_n[b]	M_w/M_n
30	72	340 000	2.45
45	90	135 000	2.75
60	96	55 000	3.4
75	99	23 800	3.75
85	99	21 800	3.9

[a,b] Reaction conditions same as in Table 2.

Rhodacarboranes (**9**) also served as catalysts for ATRP. They behaved similarly to ruthenacarboranes (Table 2). They were very active, even at a temperature as low

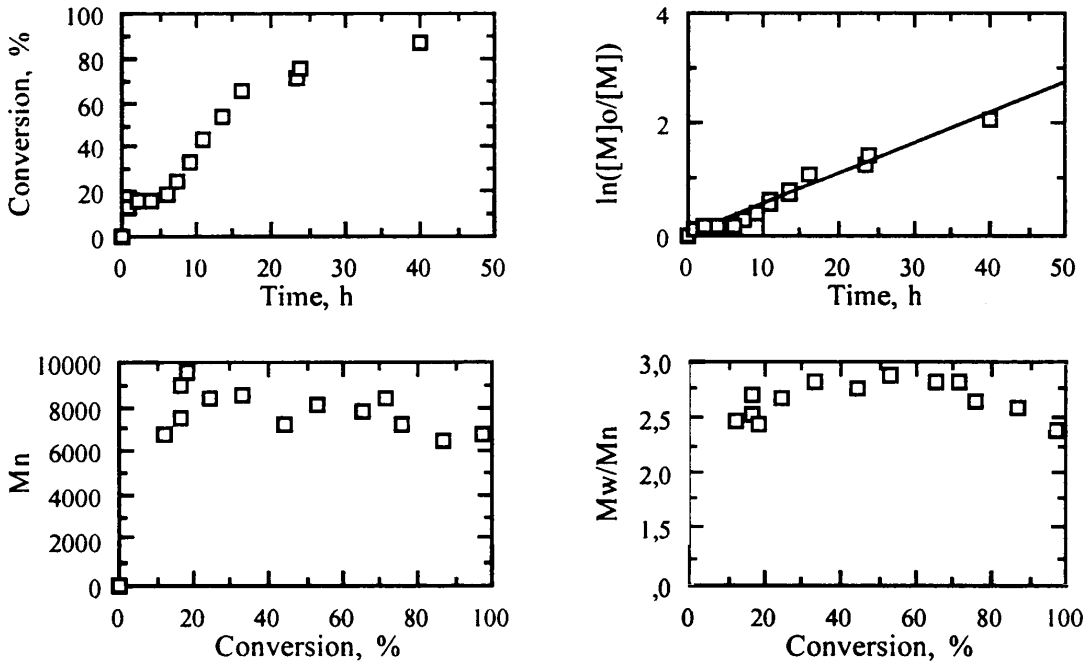

Figure 3. *Polymerization of styrene initiated by (1-bromoethyl)benzene and catalyzed by rhodacarborane* ***9a****, at 110 °C (Reaction conditions same as in Table 1).*

as 30 °C. However, whatever the temperature, polymerizations were never controlled and polydispersities were broad. Quite interesting was the influence of the temperature on both M_n and M_w/M_n (Table 3). At 30 °C, M_n was quite high (~ 350 000), indicating a low initiation efficiency. As the temperature increased, M_n decreased and M_w/M_n became broader, reaching 3.8 at 75 °C.

Rhodacarboranes also displayed unexpected reactivity profiles. As shown in Figure 3, styrene polymerization started immediately, then reached a plateau for 6-7 h corresponding to approximately 17 % conversion, after which the reaction rate was first-order with respect to the monomer (y = - 0.01124 + 0.054674 x; r^2 = 0.989). Furthermore, the polymerization was not controlled in terms of molecular weights and molecular weight distributions. M_n slightly decreased, whereas M_w/M_n remained constant (2.5-2.9) with monomer conversion (Figure 3).

Influence of the Phosphine Ligand

To further expand the potentials of the original [RuCl(Cp*)(PPh_3)$_2$] catalyst (**6**), we anticipated that the dynamic equilibration between active propagating radicals and dormant species (as sketched in Scheme 2) should also be fine-tuned through modification of the phosphine ligands. Thus, we replaced the PPh_3 ligands in complex **6** by isosteric *p*-substituted triarylphosphines so as to modify the electronic properties of the phosphine while maintaining the cone angle constant at 145°. Two phosphines were selected on the basis of their electron-donating ability: tris(4-trifluoromethylphenyl)phosphine and tris(4-methoxyphenyl)phosphine. The phosphine ability to donate σ electrons to the metal may be estimated by the basicity of the free ligand, expressed as the pK_a value for the conjugate acid (HPR_3^+) (*12*):

$$P(p\text{-}CF_3C_6H_4)_3\ (-1.75) < PPh_3\ (2.73) < P(p\text{-}CH_3OC_6H_4)_3\ (4.59)$$

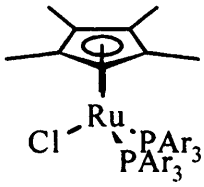

6 (Ar = C_6H_5)

10 (Ar = *p*-CF_3-C_6H_4)

11 (Ar = *p*-CH_3O-C_6H_4)

Table 4.

ATRP of Methyl Methacrylate, *n*-Butyl Acrylate, and Styrene Catalyzed by Ruthenium Pentamethylcyclopentadienyl Complexes 6, 10, and 11

Complex	*Polymer yield (%)*	M_n[d]	M_w/M_n[d]	f[c]
Methyl methacrylate[a]				
6	19	9 600	1.45	0.80
10	25	13 500	1.19	0.75
11	72	30 000	1.32	0.95
n-Butyl acrylate[b]				
6	91	36 000	1.20	0.95
10	96	37 500	1.20	0.99
11	96	37 500	1.28	0.99
Styrene[c]				
6	27	11 000	1.10	0.95
10	21	10 000	1.09	0.80
11	52	21 000	1.14	0.95

[a-c] Reaction conditions same as in Table 1.

An examination of the results collected in Table 4 reveals that the ruthenium-tris(4-methoxyphenyl)phosphine complex (**11**) was more active than the parent complex (**6**). With *n*-butyl acrylate and styrene, this was at the expense of the polydispersity which was slightly higher. With methyl methacrylate, however, the molecular weight distribution was narrower when using complex **11** (M_w/M_n = 1.32) as the catalyst instead of **6** (M_w/M_n = 1.45). In addition, the GPC curve of PMMA obtained using complex **11** was monomodal, whereas it was bimodal when using **6**. The ruthenium-tris(4-trifluoromethylphenyl)phosphine complex (**10**) displayed a reactivity similar to that of **6**. The only exception was observed with methyl methacrylate: The molecular weight distribution of the obtained PMMA was narrower with **10** (M_w/M_n = 1.19) than with **6** (M_w/M_n = 1.45).

These results indicate that electron-donating phosphines such as P(*p*-$CH_3OC_6H_4$)$_3$ exert a significant role in stabilizing the Ru(III) intermediate species (Scheme 2). They also suggest that catalyst's engineering and fine-tuning can easily be achieved by using suitable and readily available ligands.

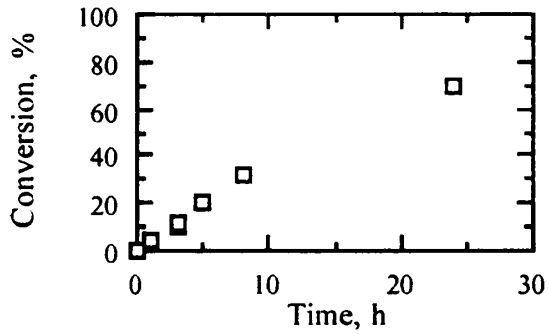

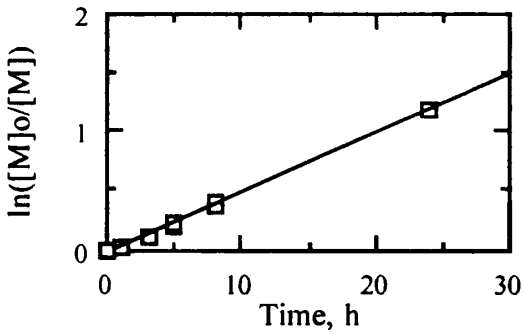

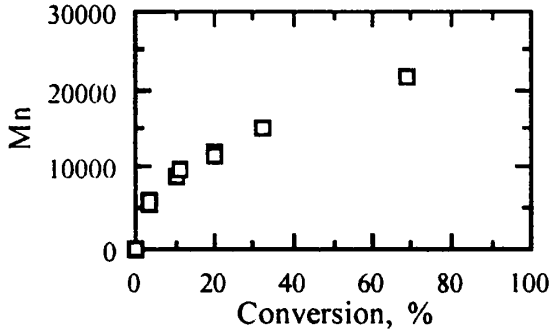

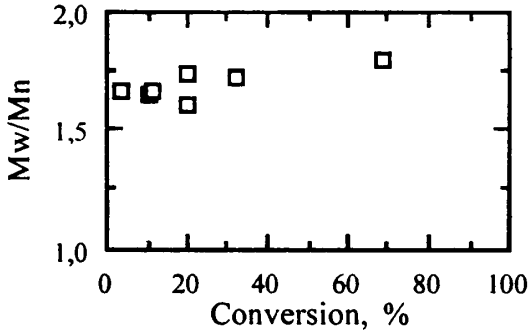

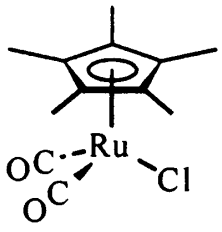

12

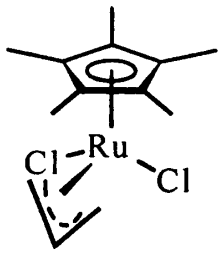

16

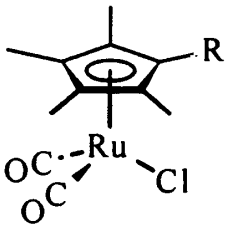

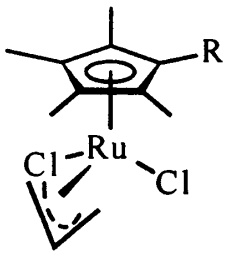

13 (R = C(O)-C_6H_5)

14 (R = CH=CH-C(O)-CH_3)

17 (R = C(O)-C_6H_5)

18 (R = CH=CH-C(O)-C_6H_5)

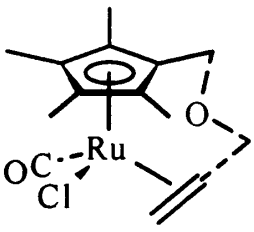

15

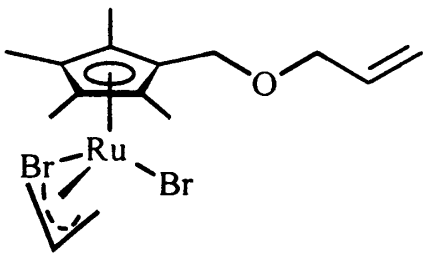

19

***Figure 4** (previous page). Polymerization of methyl methacrylate initiated by ethyl 2-bromo-2-methylpropionate and catalyzed by [RuCl(Ind)(PPh$_3$)$_2$] (7), at 85 °C, in the presence of 1 equivalent of PPh$_3$ (Reaction conditions same as in Table 1).*

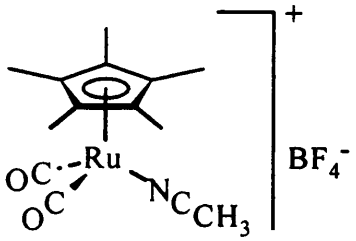

20

Table 5. ATRP of Methyl Methacrylate and Styrene Catalyzed by Ruthenium Complexes 12-20[a]

	Methyl methacrylate			Styrene		
Complex	*Polymer yield (%)*	M_n[b]	M_w/M_n	*Polymer yield (%)*	M_n[b]	M_w/M_n
12	1	-	-	50	25 000	1.85
13	1	-	-	40	56 000	3.4
14	3	145 000	2.2	21	29 000	2.05
15	16	70 000	2.05	33	20 000	1.95
16	1	9 500	1.75	30	40 000	1.95
17	4	13 000	1.7	5	2 600	2.45
18	1	31 000	1.7	1	-	-
19	1	-	-	5	12 500	1.75
20	25	480 000	2.15	38	55 000	2.1

[a, b] Same as in Table 1.

Previous studies in Kharasch chemistry (*13*) suggested that the release of a phosphine ligand from [RuCl(Cp*)(PAr$_3$)$_2$] was of utmost importance and most likely occurred prior to the activation of the dormant species by the unsaturated ruthenium center. With this in mind, kinetics of the polymerization of MMA involving [RuCl(Ind)(PPh$_3$)$_2$] in the presence of an excess of PPh$_3$ were undertaken. In the presence of 1 equivalent of PPh$_3$ with respect to ruthenium (Figure 4), the polymerization was slower (k_{app} = 1.38 x 10^{-5} s^{-1}) than without added PPh$_3$ (k_{app} = 2.16 x 10^{-5} s^{-1}). The semi logarithmic plot of MMA conversion against time was linear (y = - 0.018232 + 0.049556 x; r^2 = 0.999) throughout the reaction. Interestingly, the M_n vs. conversion plot showed a significant deviation from linearity, and the MWDs became broader (~ 1.7 instead of 1.3 without added PPh$_3$).

In order to assess the importance of the release of the phosphine ligand, we replaced PPh$_3$ by the carbonyl ligand, which forms stronger bonds to metal centers than most phosphines. Thus, we investigated a new class of ruthenium(II) complexes, [RuCl(Cp$^{\#}$)(CO)$_2$], bearing two carbon monoxide ligands and Cp* or

various substituents tethered $Cp^{\#}$ ligands (Table 5). Complexes **12-15** and their cationic derivative (**20**) proved to be poorly active, and molecular weight distributions were broad. As expected, related ruthenium(IV) complexes (**16-19**) were practically inactive under ATRP conditions.

Conclusions

In exploring the reactivity of many analogous $[RuCl(Cp^{\#})(PR_3)_2]$ complexes for ATRP of methyl methacrylate, *n*-butyl acrylate, and styrene, it was found that $[RuCl(Cp^*)(PPh_3)_2]$ and $[RuCl(Ind)(PPh_3)_2]$ were highly efficient catalysts. Highly electron-donating ligands such as carboranes led to inefficient catalysts. As indicated by several experimental facts, the mechanism would involve the dissociation of a phosphine ligand, giving rise to a 16-electron species at which activation of the carbon-halogen bond of the initiator and of the dormant species could take place.

Acknowledgments

This work was financially supported by a grant-in-aid (O.T.) joined to the project MAT98-0921 from CICYT (Spain). Part of this work has also been carried out in the framework of the COST D17/0006/00 and TMR-HPRN CT 2000-10 'Polycat' programs (European Union). The Belgian team is also grateful to the 'Fonds National de la Recherche Scientifique' (F.N.R.S.), Brussels, for the purchase of major instrumentation, and the 'Région wallonne' (Programme FIRST Europe) for a fellowship to A.R.

References

1. Kato, M.; Kamigaito, M.; Sawamoto, M.; Higashimura, T. *Macromolecules* **1995**, *28*, 1721.
2. Wang, J.-S.; Matyjaszewski, K. *J. Am. Chem. Soc.* **1995**, *117*, 5614.
3. (a) Sawamoto, M.; Kamigaito, M. *Chemtech* **1999**, *29(6)*, 30. (b) Kamigaito, M.; Ando, T.; Sawamoto, M. *Chem. Rev.* **2001**, *101*, 3689.
4. (a) Hamasaki, S.; Kamigaito, M.; Sawamoto, M. *Macromolecules* **2002**, *35*, 2934. (b) Hamasaki, S.; Sawauchi, C.; Kamigaito, M.; Sawamoto, M. *J. Polym. Sci., Part A: Polym. Chem.* **2002**, *40*, 617.
5. (a) Sawamoto, M.; Kamigaito, M.; Ando, T. *Macro Group UK*, University of Warwick, July 29th - August 1st, 2002, IL42. (b) Kamigaito, M.; Ando, T.; Sawamoto, M. *224th ACS National Meeting*, August 18-22, 2002, POLY 34. (c) Kamigaito, M.; Ando, T.; Sawamoto, M. *Polym. Prepr.* **2002**, *43(2)*, 3.
6. (a) Simal, F.; Demonceau, A.; Noels, A. F. *Angew. Chem.* **1999**, *111*, 559; *Angew. Chem. Int. Ed.* **1999**, *38*, 538. (b) Simal, F.; Jan, D.; Delaude, L.; Demonceau, A.; Spirlet, M.-R.; Noels, A. F. *Can. J. Chem.* **2001**, *79*, 529.
7. Simal, F.; Delfosse, S.; Demonceau, A.; Noels, A. F.; Denk, K.; Kohl, F. J.; Weskamp, T.; Herrmann, W. A. *Chem. Eur. J.* **2002**, *8*, 3047.
8. Simal, F. PhD Thesis, University of Liège, **2000**.
9. White, D.; Coville, N. J. *Adv. Organomet. Chem.* **1994**, *36*, 95.
10. Calhorda, M. J.; Romão, C. C.; Veiros, L. F. *Chem. Eur. J.* **2002**, *8*, 868.
11. Watanabe, Y.; Ando, T.; Kamigaito, M.; Sawamoto, M. *Macromolecules* **2001**, *34*, 4370.
12. Rahman, Md. M.; Liu, H.-Y.; Eriks, K.; Prock, A.; Giering, W. P. *Organometallics* **1989**, *8*, 1.
13. (a) Simal, F.; Wlodarczak, L.; Demonceau, A.; Noels, A. F. *Tetrahedron Lett.* **2000**, *41*, 6071. (b) Simal, F.; Wlodarczak, L.; Demonceau, A.; Noels, A. F. *Eur. J. Org. Chem.* **2001**, 2689.

CONTROLLED RADICAL POLYMERISATION CATALYSED BY RUTHENIUM COMPLEXES. VARIATIONS ON Ru-Cp#

Sébastien Delfosse,[a] *Bernard Guillaume,*[a] *Aurore Richel,*[a] *Albert Demonceau,*[a]* *Alfred F. Noels,*[a] *Oscar Tutusaus,*[b] *Rosario Núñez,*[b] *Clara Viñas,*[b] *Francesc Teixidor,*[b] *and Janusz Baran*[c]

[a] Laboratory of Macromolecular Chemistry and Organic Catalysis
University of Liège, Sart-Tilman (B.6a), B-4000 Liège, Belgium
[b] Institut de Ciència de Materials de Barcelona, CSIC
Campus de Bellaterra, Cerdanyola, 08193 Barcelona, Spain
[c] Institute of Fundamental Chemistry, Technical University of Szczecin
Al. Piastów 42, PL-70065 Szczecin, Poland

Introduction

Sawamoto *et al.*[1] and Matyjaszewski *et al.*[2] first reported on the atom transfer radical polymerisation (ATRP) of vinyl monomers using catalytic systems based on ruthenium and copper, respectively.[3] The best copper-based systems generally contained nitrogen ligands, such as bipyridine, multidentate amines, and Schiff bases, whereas $RuCl_2(PPh_3)_3$, the first ruthenium catalyst proposed by Sawamoto *et al.*, required the addition of a Lewis acid, *i.e.*, MeAl(2,6-di-*tert*-butylphenoxide)$_2$ or Al(O-*i*Pr)$_3$ to become active. Recently, we reported on the exceptional efficacy of new catalytic systems based on $[RuCl_2(p\text{-cymene})(PR_3)]$ complexes **1** (*p*-cymene = 4-isopropyltoluene) to promote the controlled free-radical polymerisation of vinyl monomers *without* cocatalyst activation.[4] More recently, we also reported that various ruthenium-alkylidene complexes commonly used for olefin metathesis (Grubbs' complex (**2a**) and Herrmann's complexes (**2b** and **2c**)) were also efficient catalyst precursors for ATRP.[5]

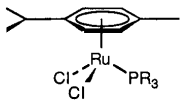

1

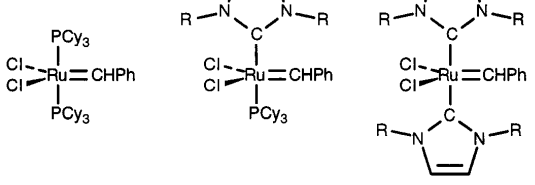

2a **2b** **2c**

Meanwhile, other ruthenium complexes were shown to mediate the controlled radical polymerisation of methyl methacrylate and styrene, namely PPh_3-based ruthenium(II) hydrides, $RuH_2(PPh_3)_4$[6] and ruthenium-carborane complexes.[7]

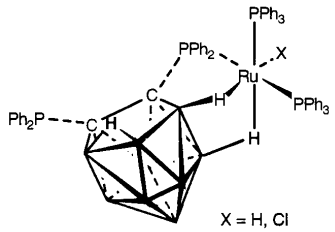

Recently, Sawamoto[8] and us[9] found almost simultaneously that 18-electron half-metallocene-type ruthenium complexes **3-5** led to the controlled radical

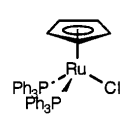

3

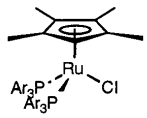

4

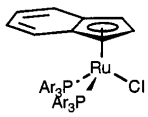

5

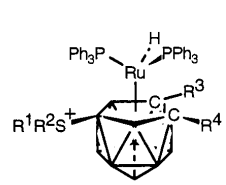

6

polymerisation of vinyl monomers. In this paper, we present some studies on the scope and limitations of stable half-sandwich (**3-6**) and sandwich ruthenium (**7-9**) complexes as potential catalysts for the ATRP of vinyl monomers.

Experimental Section

Materials. $[RuCl(Cp)(PPh_3)_2]$ (**3**), $[RuCl(Ind)(PPh_3)_2]$ (**5**, Ar = Ph), and $[Ru(Cp^*)_2]$ were used as received from Strem. $[Ru(Cp)_2]$ was used as received from Aldrich. $[RuCl(Cp^*)(PAr_3)_2]$ complexes (**4**, Ar = C_6H_5, *p*-$CH_3OC_6H_4$, and *p*-$CF_3C_6H_4$) were synthesised according to the literature.[10] $[RuCl(Ind)(P(p\text{-}CH_3OC_6H_4)_3)_2]$,[11a] **6**,[11b] and **9**[11a] were synthesised by B.G. and O.T. The monomers (methyl methacrylate, styrene, and *n*-butyl acrylate), the initiators (ethyl 2-bromo-2-methylpropionate, ethyl 2-bromopropionate, and (1-bromoethyl)benzene), and the solvent (toluene) were dried using conventional procedures,[12] distilled under nitrogen or under reduced pressure, and stored under N_2 at -20 °C.

Polymerisation. All of the experiments were conducted using standard Schlenk techniques. In a typical experiment, the ruthenium complex (0.0117 mmol) and a magnetic bar were introduced in a glass tube which was then closed by a three-way stopcock and degassed by applying three vacuum/nitrogen cycles. The monomer (methyl methacrylate, 1 ml, 9.35 mmol; styrene, 1 ml, 8.73 mmol, *n*-butyl acrylate, 1 ml, 6.98 mmol), and the initiator (0.1 M in toluene, 0.234 ml) were added successively under nitrogen with a syringe. The reaction mixture was heated for 16 h at 85 °C. Monomer conversion was determined by withdrawing samples at regular time intervals from the reaction mixture and analysing them by GLC, or from the amount of polymer precipitated in heptane (PMMA) or methanol (PS). The recovered polymer was dried overnight at 80 °C under high vacuum and weighed.

Characterisation. Molecular weight and molecular weight distributions were determined by SEC in THF at 40 °C using a Hewlett-Packard 1090 liquid chromatograph equipped with a Hewlett-Packard 1037A refractive index detector. PMMA and PS standards (Polymer Laboratories) were used for calibration. Before SEC analysis, the polymer solutions were filtered through Al_2O_3 plugs.

Table 1. Polymerisation of *n*-Butyl Acrylate Initiated by Ethyl 2-Bromo-2-propionate and Catalysed by Ruthenium Complexes 1-5, at 85 °C[a]

Complex	Polymer yield %	M_n[b]	M_w/M_n	f[c]
1 (R = Cy)	80	37 500	1.95	0.8
1 (R = *i*Pr)	81	32 000	1.40	0.95
2a	82	43 500	1.75	0.7
3	4	1 500	1.35	1.0
4 (Ar = C_6H_5)	91	36 000	1.20	0.95
4 (Ar = *p*-$CH_3OC_6H_4$)	96	37 500	1.20	1.0
4 (Ar = *p*-$CF_3C_6H_4$)	96	37 500	1.28	1.0
5 (Ar = C_6H_5)	66	35 000	2.3	0.7
5 (Ar = *p*-$CH_3OC_6H_4$)	54	42 500	2.6	0.5

[a] Reaction conditions: catalyst, 0.0117 mmol; *n*-butyl acrylate, 1 ml; initiator, 0.0234 mmol; polymerisation time, 16 h (see the Experimental Section for details). [b] Size exclusion chromatography calibrated with PMMA standards. [c] Initiation efficiency $f = M_{n,theor.}/M_{n,exp.}$ with $M_{n,theor.} = ([n\text{BA}]_0/[\text{initiator}]_0) \times M_w(n\text{BA}) \times$ conversion.

* Corresponding author. Tel.: ++32 4366 3495; fax: ++32 4366 3497; e-mail: A.Demonceau@ulg.ac.be

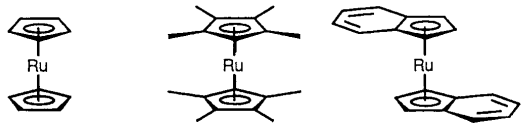

7 8 9

Table 2. Polymerisation of Methyl Methacrylate Initiated by Ethyl 2-Bromo-2-methylpropionate and Catalysed by Ruthenocenes 7-9, at 85 °C[a]

Ruthenocene	Polymer yield %	M_n[b]	M_w/M_n	f[c]
7	38	605 000	2.6	0.02
8	19	445 000	2.65	0.02
9	40	675 000	2.0	0.02

[a] Reaction conditions: catalyst, 0.0117 mmol; MMA, 1 ml; initiator (ethyl 2-bromo-2-methylpropionate), 0.0234 mmol; polymerisation time, 16 h (see the Experimental Section for details). [b] Size exclusion chromatography calibrated with PMMA standards. [c] Initiation efficiency $f = M_{n,theor.}/M_{n,exp.}$ with $M_{n,theor.} = ([MMA]_0/[initiator]_0) \times M_w(MMA) \times$ conversion.

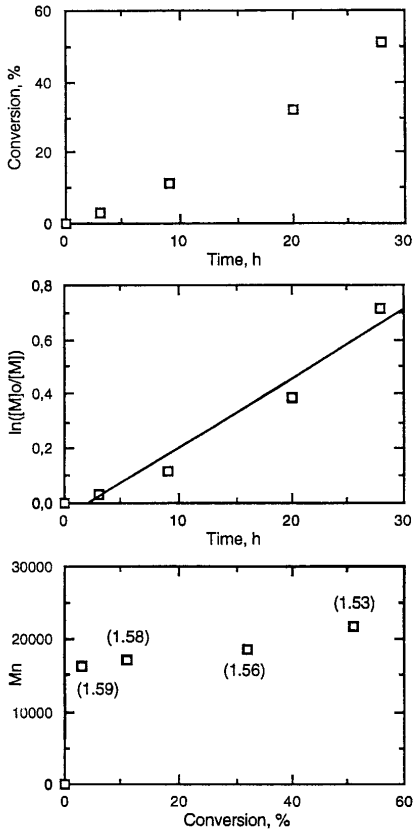

Figure 1. Time dependence of conversion and $\ln([M]_0/[M])$ where $[M]_0$ and $[M]$ are the styrene concentration at times 0 and t (y = - 5.1329 10^{-2} + 2.5044 10^{-2} x; r^2 = 0.961); and styrene conversion dependence of the polystyrene molecular weight M_n and polydispersity M_w/M_n. Reaction conditions: styrene, 1 ml, 8.73 mmol; (1-bromoethyl)benzene (0.1 M in toluene, 0.234 ml); $Ru(Ind)_2$ (**9**), 3.9 mg, 0.0117 mmol; temperature, 110 °C.

Results and Discussion

Investigations were undertaken with the aim to determine how the electronic and steric properties of the ligands affect catalyst activity. Ruthenium complexes of the type $[RuX(Cp^{\#})(PAr_3)_2]$ (X = Cl, H; $Cp^{\#}$ = Cp, Cp*, indenyl, and carboranyl) (**3-6**) were chosen as potential catalysts for two reasons: (1) upon $Cp^{\#}$ ligand substitution, it is expected to modify the electronic contributions in these systems. The higher electron donating ability of Cp* compared to Cp is well-established, and the capacity of carboranyl ligands ($[C_2B_9H_{11}]^{2-}$) to stabilise uncommon and high oxidation states of the metals as well. (2) On the other hand, $Cp^{\#}$ substitution also results in changing the steric properties of the ligands, which are expressed by the cone angle. In this way, Cp* is obviously bulkier than Cp and, most probably, than the carboranyl ligand $[C_2B_9H_{11}]^{2-}$, although the relative size of the latter compared to Cp and Cp* is still a question under debate. The indenyl ligand poses a more complex problem since it is known to undergo a facile metal ring slippage from η^5- to η^3-coordination, leading to the creation of a vacant coordination site on the metal to host an entering ligand or substrate.

Ruthenium complexes **3-6** are active catalysts for the polymerisation of methyl methacrylate and styrene, and their efficiency markedly depends on the $Cp^{\#}$ ligand and on the phosphine used. More interesting is the observation that Ru-Cp* complexes (**4**) are the first ruthenium-based complexes to mediate the controlled radical polymerisation of *n*-butyl acrylate (Table 1). Ruthenium complexes previously reported, such as $[RuCl_2(PPh_3)_3]$, $[RuCl_2(p\text{-cymene})(PR_3)]$ (**1**), and ruthenium alkylidenes (**2**), are inefficient for that reaction. Interestingly enough, with *n*-butyl acrylate, the molecular weight distribution dropped from 1.9 to 1.4 simply by the use of $PiPr_3$ as the phosphine (instead of PCy_3), demonstrating therefore the importance of the ligand sphere. The pivotal role of the ligands is also illustrated by the use of $[RuCl(Ind)(PAr_3)_2]$ (**5**), which are effective for methyl methacrylate and styrene but not acrylates. Furthermore, polymerisations catalysed by ruthenium-carborane complexes (**6**) are extremely fast and totally uncontrolled.

In order to address the importance of ring-slippage in ruthenium-indenyl complexes (**5**), $Ru(Ind)_2$ (**9**) was synthesised and its activity was compared to that of $Ru(Cp)_2$ (**7**) and $Ru(Cp^*)_2$ (**8**) (Table 2). These sandwich complexes displayed similar reactivities, which likely rules out the possibility of ring-slippage. The polymerisations were poorly controlled with MMA, and uncontrolled with styrene (Figure 1).

Acknowledgement. This work has been carried out in the framework of the COST D17/00600 and TMR-HPRN CT 2000-10 "Polycat" programmes. The Belgian team is grateful to the "Fonds National de la Recherche Scientifique" (F.N.R.S.), Brussels, for the purchase of major instrumentation, and the "Région wallonne" (FIRST Europe programme) for a fellowship to A. Richel. This work was also supported by CIRYT (Spain) (project MAT98-0921).

References

(1) Kato, M.; Kamigaito, M.; Sawamoto, M.; Higashimura, T. *Macromolecules* **1995**, *28*, 1721-1723.
(2) (a) Wang, J.-S.; Matyjaszewski, K. *J. Am. Chem. Soc.* **1995**, *117*, 5614-5615. (b) Wang, J.-S.; Matyjaszewski, K. *Macromolecules* **1995**, *28*, 7901-7910.
(3) For recent reviews, see: (a) Sawamoto, M.; Kamigaito, M. *Chemtech* **1999**, *29* (6), 30-38. (b) Matyjaszewski, K. *Chem. Eur. J.* **1999**, *5*, 3095-3102. (c) Matyjaszewski, K.; Xia, J. *Chem. Rev.* **2001**, *101*, 2921-2990. (d) Kamigaito, M.; Ando, T.; Sawamoto, M. *Chem. Rev.* **2001**, *101*, 3689-3745.
(4) Simal, F.; Demonceau, A.; Noels, A. F. *Angew. Chem.* **1999**, *111*, 559-562; *Angew. Chem., Int. Ed.* **1999**, *38*, 538-540.
(5) Simal, F.; Delfosse, S.; Demonceau, A.; Noels, A. F.; Denk, K.; Kohl, F. J.; Weskamp, T.; Herrmann, W. A. *Chem. Eur. J.* **2002**, *8*, in press.
(6) Takahashi, H.; Ando, T.; Kamigaito, M.; Sawamoto, M. *Macromolecules* **1999**, *32*, 6461-6465.
(7) Simal, F.; Sebille, S.; Demonceau, A.; Noels, A. F.; Núñez, R.; Abad, M.; Teixidor, F.; Viñas, C. *Tetrahedron Lett.* **2000**, *41*, 5347-5351.
(8) Watanabe, Y.; Ando, T.; Kamigaito, M.; Sawamoto, M. *Macromolecules* **2001**, *34*, 4370-4374.
(9) Simal, F. PhD Thesis, University of Liège, 2000.
(10) (a) Fagan, P. J.; Mahoney, W. S.; Calabrese, J. C.; Williams, I. D. *Organometallics* **1990**, *9*, 1843-1852. (b) Chinn, M. S.; Heinekey, D. M. *J. Am. Chem. Soc.* **1990**, *112*, 5166-5175. (c) Serron, S. A.; Luo, L.; Li, C.; Cucullu, M. E.; Stevens, E. D.; Nolan, S. P. *Organometallics* **1995**, *14*, 5290-5297.
(11) Unpublished results. (a) B.G. (b) O.T.
(12) (a) Perrin, D. D.; Armarego, W. L. F. *Purification of Laboratory Chemicals*, 3rd Edition, Pergamon Press, 1988. (b) Furniss, B. S.; Hannaford, A. J.; Smith, P. W. G.; Tatchell, A. R. *Vogel's Textbook of Practical Organic Chemistry*, 5th Edition, Longman Scientific and Technical, 1989.